Robust Control Design for DC/DC Converter and its Hardware Implementation

Submitted by:

Hammad Sami Khan

Supervised by:

Dr. Attaullah Y. Memon PN

THESIS

Submitted to:

Department of Electronic and Power Engineering

Pakistan Navy Engineering College Karachi

National University of Science and Technology, Islamabad Pakistan

In fulfillment of requirement for the award of the degree of

MASTER OF SCIENCE IN ELECTRICAL ENGINEERING

With Specialization in Control Engineering

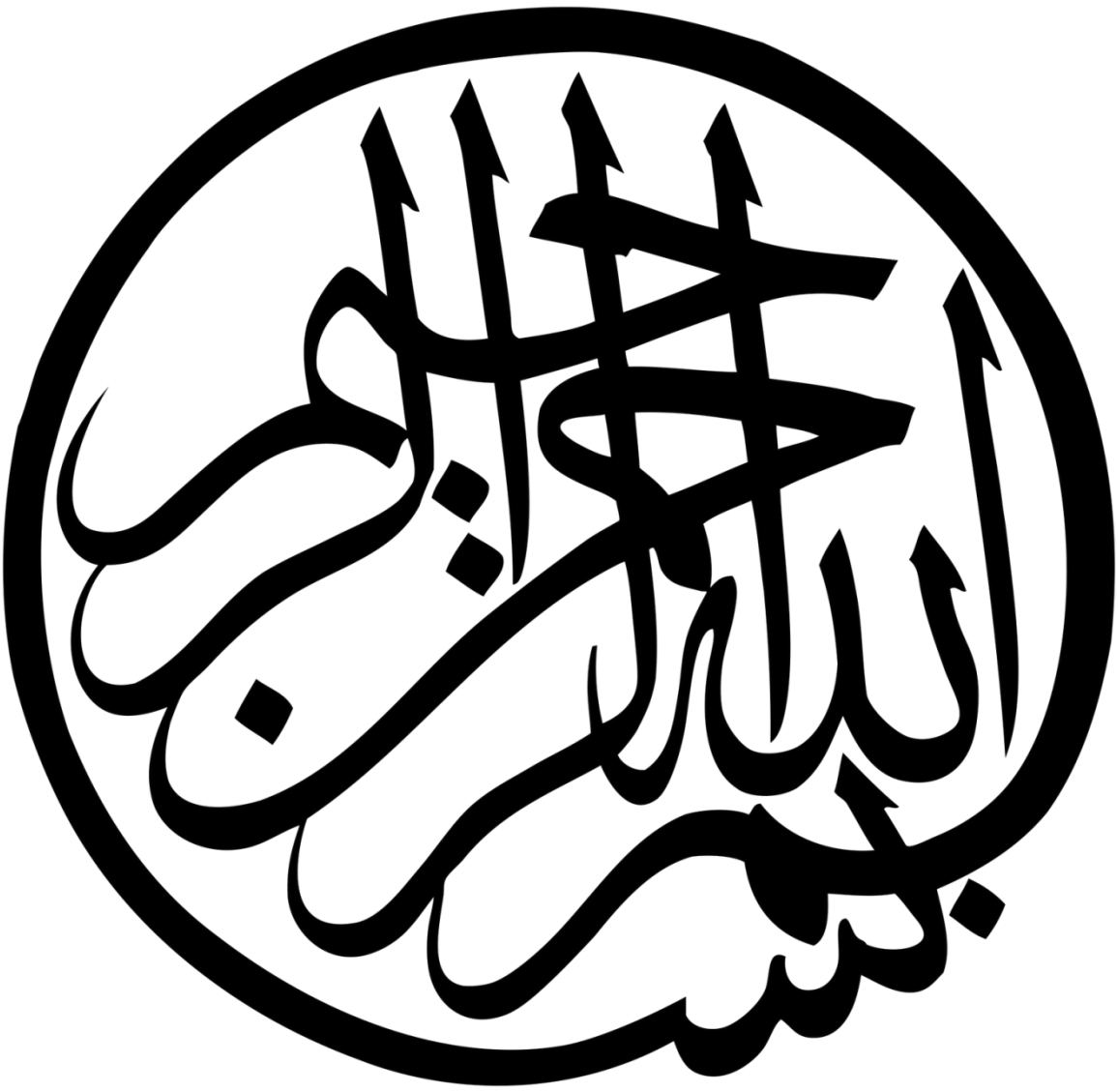
بسم الله الرحمن الرحيم

Abstract

A robust control technique namely Sliding Mode Controller is proposed for DC/DC Boost Converter to maintain the desired output voltage in the presence of parametric variations and external disturbances. The proposed design technique utilizes the current-mode control strategy in order to effectively address parametric variations as well as sensitivity to noise. However this essentially requires use of a current sensor. A sensorless control strategy is thus proposed using a nonlinear observer that estimates the current. The striking feature of the proposed strategy is that it eliminates the need of a current sensor (hardware) thereby reducing the overall cost as well as minimizing system complexity which helps in hardware implementation of the control design. The efficacy of the proposed scheme is verified by simulation. It is shown that the proposed sensorless control scheme is robust to variations in input and load as well as to the noise present in the operational environment. The proposed control scheme is then implemented on a Field Programmable Gate Array (FPGA) and a FPGA-In-the-Loop (FIL) simulation is carried out to demonstrate the efficient hardware implementation/realization of the proposed control scheme for a DC/DC Boost Converter.

Acknowledgement

I am thankful to Almighty ALLAH, the most merciful and beneficent, for His blessings that enable us to recognize and pursue knowledge in life. My sincere gratitude to my supervisor Dr. Attaullah Y. Memon PN, Assistant Professor, Department of Electronic and Power Engineering at PN Engineering College, NUST. I consider myself very lucky and honored to have him as my supervisor. I thank him for his unprecedented attention and patience throughout the thesis work. I admire him as a teacher and as a person.

In addition to above, I am also thankful to the guidance committee comprising of following faculty members who led me to achieve my target:

- Dr. Aleem Mushtaq PN
- Dr. Naeem Abbas

I want to take this opportunity to thank my parents, my siblings and my friends. Thank you for your prayers, love, encouragement, patience… Thank you for everything.

Contents

List of Figures

List of Tables

List of symbols

$\mathbf{V_O}$	Output Voltage of DC/DC Converter
$\mathbf{V_{ref}}$	Reference Voltage of DC/DC Converter
$\mathbf{V_{in}}$	Input Voltage of DC/DC Converter
$\mathbf{I_L}$	Inductor Current
U	Input Control Signal(0 or 1)
R	Load resistance
L	Inductor Value
C	Capacitor Value
E	Error (difference of measured and reference Voltage)
PI	Proportional Integral Controller

FIL	FPGA-IN-THE-LOOP
$\mathbf{I_L}$*	Desired Inductor Current
Sgn	Signum Function
$\boldsymbol{l_1}$,$\boldsymbol{l_2}$	Sliding Mode Observer Gains
$\boldsymbol{h_1}$,$\boldsymbol{h_2}$	High Gain Observer Gains
$\mathbf{\hat{i}_L}$	Observed Inductor Current
$\mathbf{\hat{V}_o}$	Observed Output Voltage
$\mathbf{\tilde{i}_L}$	Difference between observed and measured Inductor Current
$\mathbf{\tilde{V}_o}$	Difference between observed and measured Output Voltage
$\boldsymbol{\alpha_1}$, $\boldsymbol{\alpha_2}$	Alpha
E	Epsilon

Chapter 1 Introduction

1.1 Rationale

DC/DC Converters are the circuits that convert one voltage level to another voltage level as required for the particular application. These have wide applications in the portable devices such as cellular phones and laptops. These are also used in the circuits for the renewable sources to maintain the desired output voltage in order to charge batteries with variable input voltage while trading off current. It also has wide usage in the electric automobiles.

DC/DC Converters can be used either to decrease or increase the output voltage based on the application requirements. It is classified into three major categories.

1.1.1 Buck Converter

This DC/DC Power Converter steps down the input voltage to the desired voltage by stepping up current. As compared to linear regulators, this switching converter provides better efficiency by stepping up the current rather than dissipating power in the form of heat.

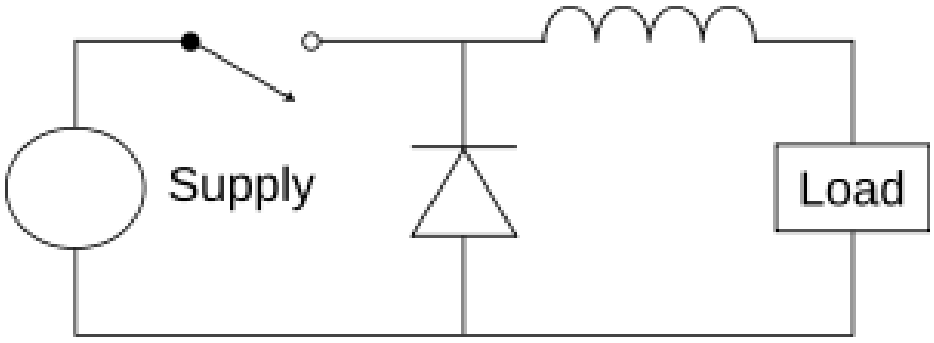

Figure 1.1: Buck Converter Topology

1.1.2 Boost Converter

This DC/DC Power Converter steps up the input voltage to the desired voltage by lowering current. It is utilized in the cases where source voltage is less than the required voltage for load.

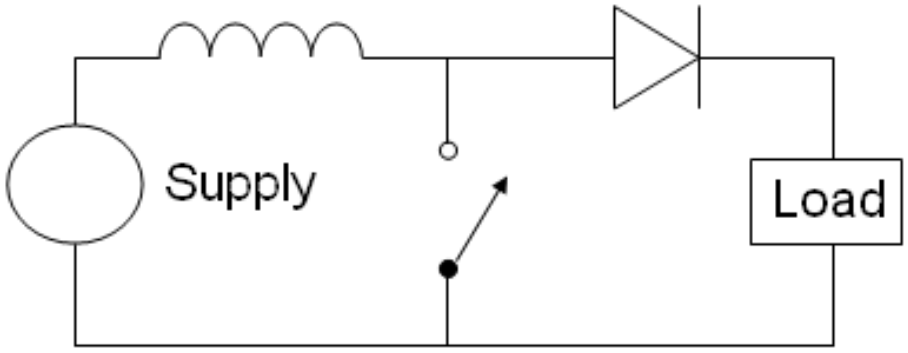

Figure 1.2: Boost Converter Topology

1.1.3 Buck-Boost Converter

As the name depicts, it is a buck converter combined with the boost converter. Therefore, the desired output voltage can either be greater or less than the input source based on application specification. This can be done by trading off source current.

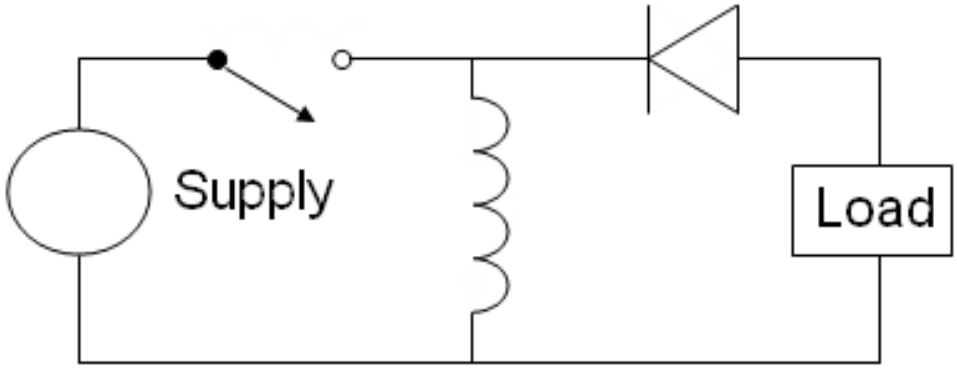

Figure 1.3: Buck-Boost Converter Topology

1.2 Aim of the Thesis

The main objective of this thesis is the FPGA implementation of a robust sensor-less control design technique which is efficient enough to maintain the desired output voltage of the DC/DC Converter under unmodeled parametric disturbances and external perturbations. The DC/DC Boost Converter is opted as a model for this thesis. The overall task is divided into four sub-problems.

- The controller design technique must be robust and has a rapid response to uncertainties.
- The controller must be capable enough to maintain the desired output voltage, if the parasitic resistances of the actual components are incorporated in the DC/DC Converter model.
- Sensor-less control design technique must be opted to reduce hardware circuitry, production and development cost.
- The control scheme must be implemented on FPGA to verify the performance of controller on hardware speeds.
- FIL (FPGA-IN-THE-LOOP) simulation must be performed to realize the controller in hardware speeds

1.3 Contributions

The thesis has following main contributions:

- State space model of DC/DC Boost Converter is illustrated in detail. The actual circuit is also designed using Simulink tool (Sim-power) which includes parasitic resistances.
- As the system is non-linear in nature, the nonlinear robust controller named as Sliding Mode Controller is opted. Stability analysis and simulations are performed to verify its robustness and sensitivity to parametric changes of DC/DC Boost Converter.
- As the Sliding Mode Controller tracks the inductor current because of its fast response. The controller will take inductor current as feedback which requires

current sensor. As a result, the addition of current sensor increases system's hardware complexity as well as overall cost of the design. Hence, sensor-less control design technique, incorporating non-linear observers such as Sliding Mode Observer and High Gain Observer, are introduced to estimate the inductor current.

- The hardware realization of the controller is also verified by implementing the sensor-less control design technique presented in this thesis on FPGA.
- FPGA-IN-THE-LOOP simulations are performed to ensure the robustness of the control scheme running on hardware speeds with respect to variations or noise in input voltage, load variations and effect of parasitic resistances.

1.4 Thesis Organization

The presented thesis is organized into six chapters, with a brief description given as follows:

- Chapter 1 provides a brief introduction to the research problem, aims thesis and objectives.
- Chapter 2 gives a brief literature review of the control problems and schemes/techniques developed for DC/DC Boost Converter. The mathematical model for the DC/DC Boost Converter is also presented.
- Chapter 3 discusses the possible control design techniques for DC/DC Boost Converter. The most suitable non-linear robust technique will be presented. The stability analysis of the controller will also be presented. The simulation results which depict control technique's robustness by using MATLAB/Simulink® will also be presented.
- Chapter 4 discusses the sensor less implementation techniques to estimate the unknown states. In this chapter, two non-linear observers will be discussed. Simulation results will be presented for the respective observers to prove the robustness of the observers with respect to the variations in parameters such as load and input voltage.

- Chapter 5 presents the FPGA implementation of the control technique. Implementation aspects are also discussed in this chapter. The The FPGA-IN-THE-LOOP(FIL) simulation setup is presented. The FIL simulation results will be presented to show the performance of the control scheme on hardware speeds.
- Chapter 6 chalks out the underlying conclusions and possible areas for improvement and extensions.

Chapter 2 Literature Review and Proposed Mathematical Model

2.1 Introduction

This chapter provides a brief review of the control schemes in published literature. The literature shows the work that has been done in this area uptill now. The mathematical model for DC/DC Boost Converter is also discussed in detail.

2.2 A brief survey on the Control Design Problem and Implementation

DC/DC boost converters are widely used in regulated power supplies where desired voltage is greater than the supplied voltage [1]. It has many applications in battery powered systems and power harvesting. To increase output voltage, the battery powered systems need more cells but inclusion of boost converter reduces the number of cells to be stacked by increasing output voltage. For example, the motor used in HEV Toyota Prius (Model NHW 20**)** requires 500V for which it requires nearly 417 cells but only 168 cells are used in its design to boost the voltage in range of 202-500V [2]. Simple applications include powering up a 3.3V white LED using a 1.5V alkaline battery using a boost converter [2].

In past few years, numerous control techniques have been presented which can be applied to control the non-linear time invariant DC/DC Boost Converter. Nonlinear control methods are preferred over linear techniques to maintain the stability of the system under parametric changes [3][4]. In this regard, many nonlinear control design tools have been used. For instance, backstepping technique, a nonlinear control technique, is used to design current mode controller to achieve better performance [18]. Model Predictive Controller (MPC), introduced in [19], optimises a cost function without any use of online optimisation method. Sliding Mode Control (SMC) maintains system's stability under unmodeled parametric changes and external disturbances [4]. Due to its switching functionality, Sliding Mode Control scheme is considered as the best alternative to PWM based linear controllers and can be naturally implemented in Switch Mode Power Converters [8].

In general, there are two basic control mode techniques applied to control DC/DC Boost Converter which are classified as Voltage-mode control and Current-mode control. The Current-mode control is having cascaded control scheme with inner control loop, which requires precise current measurement. The required inductor current can be measured using Hall Effect sensors. These sensors introduce time varying DC bias due to remnant flux. Due to limited bandwidth, it induces delay in the control system, which can affect the stability of the system. These sensors also increase overall cost of the system [11] [13]. The current can also be measured through the resistive methods. These resistive measurement methods require noise free and more accurate differential amplifiers. As a result, these methods can increase losses to the converter and reducing its efficiency. Therefore, current transformer is the most common sensor used in the industry for measurement of current [14][15]. The current transformer is required to be connected in series with MOSFET of converter, because inductance is low frequency measurement [16]. This seems to be a low cost solution, but it adds complexities for the converter. It increases high voltage spikes across semiconductor during switching transitions. It also increases the overall inductive path of the system. It jeopardizes maximum duty cycle of the converter [10]. Therefore, due to the issues regarding the implementation of current sensors in the design, sensor-less technique is proposed. It is not only cost effective solution but also provides noise free estimation of the Inductor current.

In the past, several different sensor-less control techniques have been proposed. Since, the DC/DC Boost Converter is non-linear in nature, non-linear observers are required for estimation of the required inductor current. There are few applications in which load information is usually not available. Therefore, Adaptive Non-linear Observer is proposed because it does not require load information for Boost PFC AC/DC Converters [10]. Passivity Based Control technique has also been used in the past using Kalman like observer which allows DC/DC Converter to behave well under load variations and in the presence of noise in input voltage [17]. Improved Extended Kalman Filter (EKF) was proposed for observing inductor current and minimizes the voltage noise caused by Electromagnetic Interference (EMI) [9]. An output feedback MPC based control scheme

is proposed in [19] as a sensorless technique, which is the combination of state-feedback MPC with a Luenberger-type observer. As an alternative to linear observer, the Sliding Mode Observer is introduced in [16] to estimate the inductor current. Therefore, it is highlighted that this observer also helps in minimizing the adverse effect of chattering by a suitable choice of design parameters. Another nonlinear observer, High Gain Observer is presented in [20] to estimate the unknown state. It follows the required trajectory to estimate the unknown desired state without the help of switching functions, unlike Sliding Mode Observer which results in chattering. Chattering causes more heat dissipation and it also reduces accuracy [20].

It is well established that nonlinear control techniques provide better performance and robust solutions, but implementation of complex control techniques is not very convenient, in general[4]. Due to this reason, nonlinear based solutions have not been popular in past for converters and related applications. However, with the evolution of the fast switching devices such as FPGAs, the complex nonlinear controllers and observers can now easily be implemented with better accuracy.

FPGAs have gained popularity in past decade for the implementation of different type of designs and algorithms. It has been utilized in almost every area of application such as communication, controls, networking, image processing, digital signal processing etc. The reason for its popularity is reconfigurability, shorter time to market, parallelism and reliability. The only constraint was high cost of FPGA based solutions, which is being decreased with passing years with advancement in technology. Low cost FPGAs are now available in market for small applications. Implementation on FPGA has been considered a time taking and tedious job in past. Because of the evolution of fast prototyping tools and accelerators, the design implementation time has been reduced to hours. The Xilinx System Generator is one of the successful tools by MATLAB/SIMULINK which have been evolved in past few years for fast prototyping of the designs on FPGA [8].

2.3 Proposed Boost Converter Mathematical Model

The state space model of DC/DC boost converter is obtained using ordinary differential equations as mentioned in [1]. The basic Boost switch mode converter topology is shown in Figure 2.1.

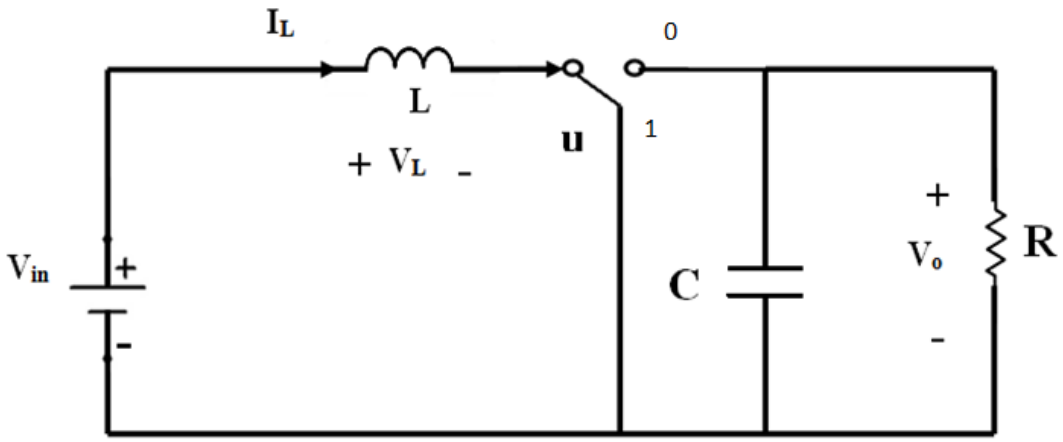

Figure 2.1: DC/DC Boost Converter Circuit

As the name implies, switch mode converter increases the output voltage. When the switch (u) is open, the circuit is separated into two parts. On the left, the input supplies the energy to the inductor while the capacitor maintains the output voltage using the previously stored energy on the output stage as shown in Figure 2.2. When the switch is off, the output receives the energy from input voltage (V_{in}) as well as the energy stored by the inductor as shown in Figure 2.3. In order to ensure constant output voltage (V_o), capacitor value is assumed very large. The operating mode considered for this switch mode controller is continuous conduction mode (CCM). In this mode of conduction, induction current (I_L) is always greater than zero i.e. I_L flows continuously.

When the switch is on (u=1) for time (t_{ON}) the inductor current (I_L) rises continuously at constant rate as shown in Figure 2.4. By applying Kirchhoff's Voltage Law along the left hand loop, it yields:

$$\frac{dI_L}{dt} = \frac{V_{in}}{L} \quad (1)$$

Since $\frac{V_{in}}{L}$ = constant and $V_L = V_{in}$ .So change in inductor current value (ΔI_L) for time (t_{ON}) is $\frac{V_{in}}{L} * t_{ON}$.

Using Kirchhoff's Current Law along the right hand loop yields as shown in Figure 2.2. $I_C = -I_R$

$$\frac{dV_o}{dt} = \frac{-V_o}{R * C} \quad (2)$$

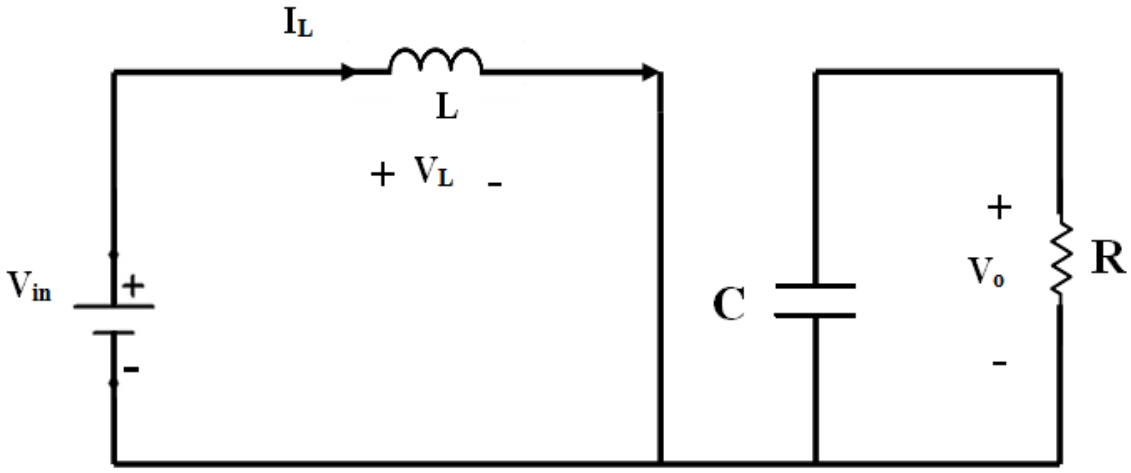

Figure 2.2: Boost Converter when Switch is on (u = 1)

When the switch is closed (u=0), the inductor voltage is negative i.e. Vin-Vo for time interval for t_{OFF} as shown in Figure 2.4. Using KVL along the left hand loop as shown in Figure 2.2.

$$\frac{dI_L}{dt} = \frac{V_{in} - V_o}{L} \quad (3)$$

Hence, the inductor current decreases for the time interval t_{OFF}. So the change in inductor current value (ΔI_L) for time (t_{OFF}) is $\frac{V_{in} - V_o}{L} * t_{OFF}$.

Using KCL along the right hand loop yields as shown in Fig. 2b.

$$I_C = I_L - I_R$$

$$\frac{dV_o}{dt} = \frac{I_L}{C} - \frac{V_o}{R * C} \quad (4)$$

Where, $I_R = \frac{V_o}{R}$ & $I_c = C * \frac{dV_o}{dt}$.

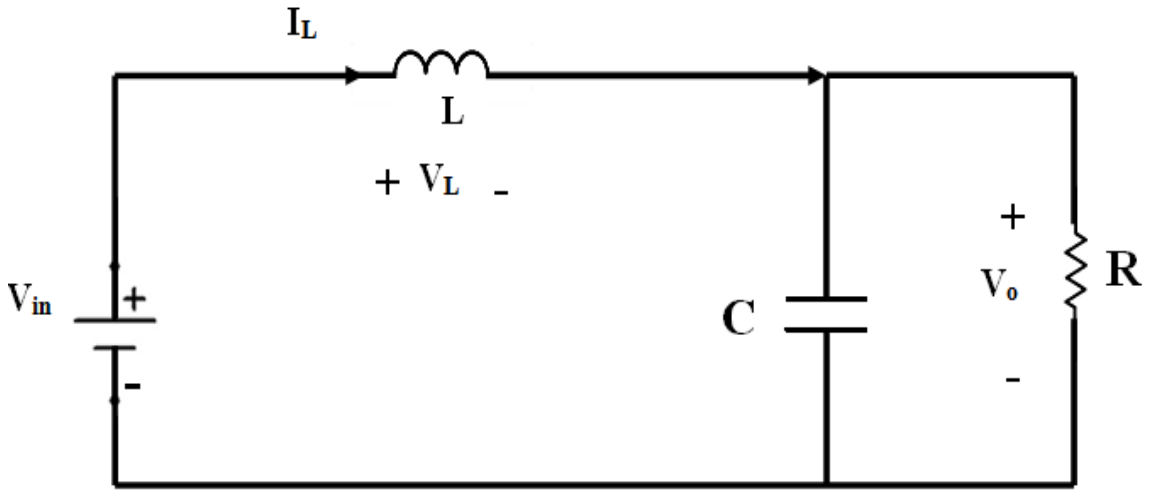

Figure 2.3: Boost Converter when Switch is on (u = 0)

As the Boost Converter is in CCM, the averaged state space equations can be determined by adding equations (1) with (3) and (2) with (4) as in [6] gives:

$$\dot{I}_L = -\frac{(1-u)V_o}{L} + \frac{V_{in}}{L} \quad (5)$$

$$\dot{V}_o = \frac{(1-u)I_L}{C} - \frac{V_O}{R * C} \tag{6}$$

In state space equation, let $x_1 = I_L$ and $x_2 = V_o$. So

$$\dot{x} = \begin{bmatrix} 0 & -\frac{(1-u)}{L} \\ \frac{(1-u)}{C} & -\frac{1}{RC} \end{bmatrix} \begin{bmatrix} x_1 \\ x_2 \end{bmatrix} + \begin{bmatrix} \frac{1}{L} \\ 0 \end{bmatrix} V_{in} \tag{7}$$

Where $x = [x_1\ x_2]^T$ and control **u** has two possible discrete values **0** or **1**.

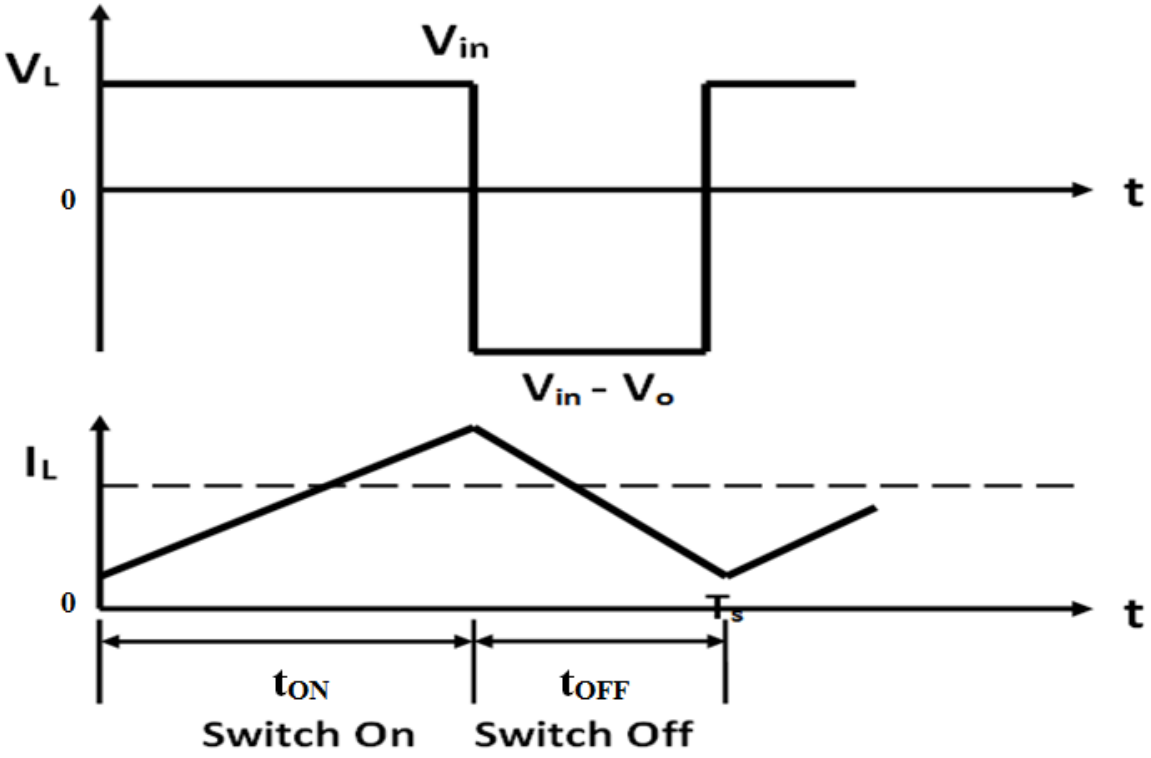

Figure 2.4: Inductor current and voltage in CCM

2.4 Conclusion

In this chapter, a brief literature review regarding the control design schemes was presented. Moreover, review clearly illustrates the work done in past and status of the research that has been done up till now in this area. The model of the Boost Converter is also presented in detail. .

Chapter 3 Control Design

3.1 Introduction

In past, several different control techniques have been proposed and implemented for the DC/DC Boost Converter. The linear control techniques were also used but are not found robust enough to maintain the desired output state under uncertain conditions. The reason is that plant is nonlinear in nature. Therefore, non-linear robust controller such as Sliding Mode controller is used to maintain the desired output voltage under uncertain parametric variations such as input voltage and load.

There are two kinds of control design techniques that can be used to control the DC/DC Boost Converter.

3.1.1 Voltage-Mode Control

The Voltage-Mode Control is the technique in which output voltage is taken as feedback and its difference with the desired voltage is fed to the controller in order to maintain the output voltage. Hence it is a single loop control technique.

3.1.2 Current-Mode Control

The Current-Mode Control is the technique in which inductor current is taken as feedback and its difference with the desired current is fed to the controller. The desired current is acquired using difference of desired voltage and output voltage as a feedback which requires another loop. Hence there is need of cascaded control structure in this regard as shown in Figure 3.1.

Since, the motion rate of inductor current is much faster than output voltage in DC/DC boost converter. Therefore the Current-Mode Control has fast system response as compared to the Voltage-Mode Control. Hence we have used Current-Mode Control in our design. Thus, according to Singular Perturbation theory, the motion separation principle is satisfied by Boost converter. Hence, cascaded control structure can be

realized and designed by having outer voltage control loop and inner current control loop [6] as shown in Figure 3.1.

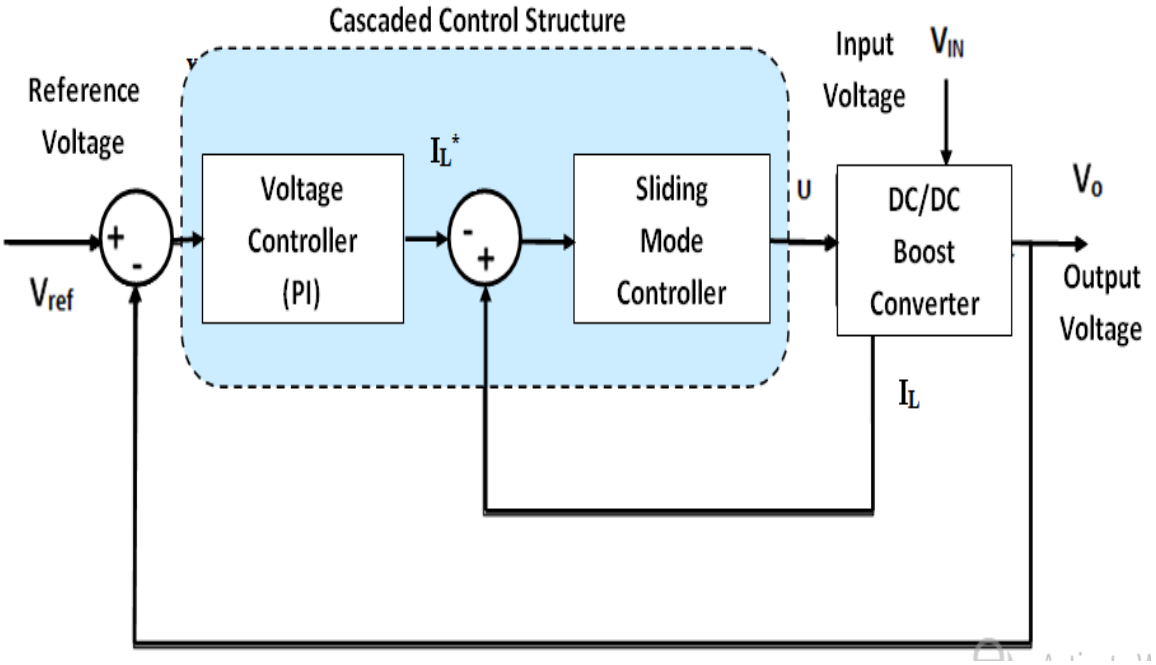

Figure 3.1: Cascaded Control Structure of Boost Converter

3.2 Outer Voltage Loop

The voltage control loop is realized using linear control techniques. Hence, the current I_L* is obtained using Proportional Integral Controller, given by

$$I_L^* = K_P e + K_I \int_0^t e dt \qquad (8)$$

Where, error $\mathbf{e = V_{ref} - V_o}$ and $\mathbf{K_P}$ and $\mathbf{K_I}$ are the proportional and integral gains respectively whose values are generally realized using trial and error methods.

3.3 Inner Current Loop

The goal of the inner control loop is to ensure that actual current I_L tracks the desired current I_L^* in the presence of uncertainties and external disturbances. This can be achieved by using a high speed switching control law (Sliding Mode Control) which renders the actual inductor current I_L to reach the predetermined path I_L^* (sliding surface) and remain in that state afterwards, while also remaining insensitive to matched un-modelled external perturbation signals and variations in plant parameters [6]. To that end, the sliding surface (switching function) for the inner loop is defined as,

$$s = \mathrm{I_L} - \mathrm{I_L^*} \tag{9}$$

In order to enforce sliding trajectory to converge to the surface (s = 0), discontinuous control law u is defined as,

$$u = \frac{1}{2}\big(1 - sgn(s)\big) \tag{10}$$

For the finite time convergence of inductor current I_L to the sliding surface I_L^*, the possible outcomes of the ideal switch *u* are

$$u = \begin{cases} 1 & for \quad s < 0 \\ 0 & for \quad s > 0 \end{cases} \tag{11}$$

We now present the analysis of the system under the proposed scheme. We first analyze the stability of current loop to verify the control structure. For this purpose, we consider the Lyapunov function candidate given as,

$$V = \frac{1}{2}s^2 \tag{12}$$

In order to show that the resulting system is stable, we require the condition

$$\dot{V} = s\dot{s} < 0$$

$$\left|2V_{in} - LI_L^{\dot{*}} - V_o\right| - V_o < 0 \tag{13}$$

It can be noted that with I_L (0) ≥ 0 and V_O (0) ≥ 0, the trajectory reach the sliding surface in finite time and remain thereafter. After sliding surface is reached (s ≈ 0), the inductor current approaches the desired current i.e $I_L \approx I_L^*$ and rate of change of desired and actual inductor current approaches to zero i.e. $\dot{I}_L \approx I_L^{\dot{*}} \approx 0$. Since, the inductor value is very small, the attraction domain for the sliding manifold is given by,

$$V_O > V_{in} > 0 \tag{14}$$

It is evident from equation (14) that the system remains stable until output voltage is greater than the input voltage.

3.4 Simulation and Results of Control Design Technique

Simulations are performed to verify the performance and robustness of the Sliding Mode Controller to external disturbances and parametric changes. Firstly the scenario of inner control loop is shown. Secondly, scenarios are developed and verified through simulations that controller is robust enough to remain stable in the presence of the unmodeled parametric changes. Moreover, in the presence of external disturbances and noises, controller remains least sensitive.

3.4.1 Simulation of Inner Control Loop

To verify the control law namely Sliding Mode Control designed in the previous section for inner control loop as shown in Figure 3.2, simulations are performed for the DC/DC boost converter model. The target of this simulation is to test that inductor current (I_L) must approach the desired current (I_L^*).

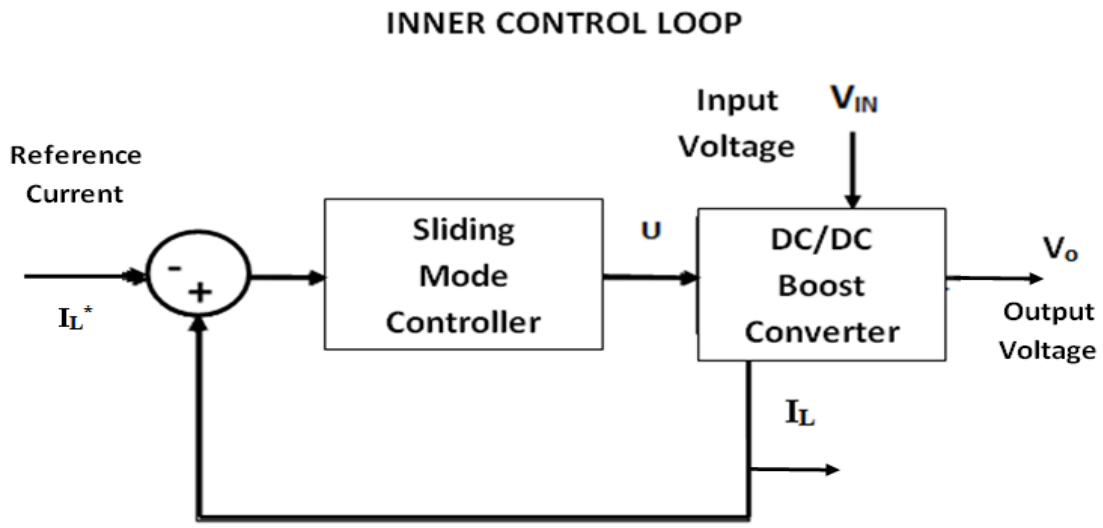

Figure 3.2: Inner Control Loop

Considering the desired inductor current I_L* changesfrom 60mA to 50mA at time 0.07sec with the parameters: V_{in} = 5V, L = 330mH, R = 820Ω and C = 4.7uF. Figure 3.3 shows that I_L converges rapidly to the desired current I_L* and V_o approaches to 12V.

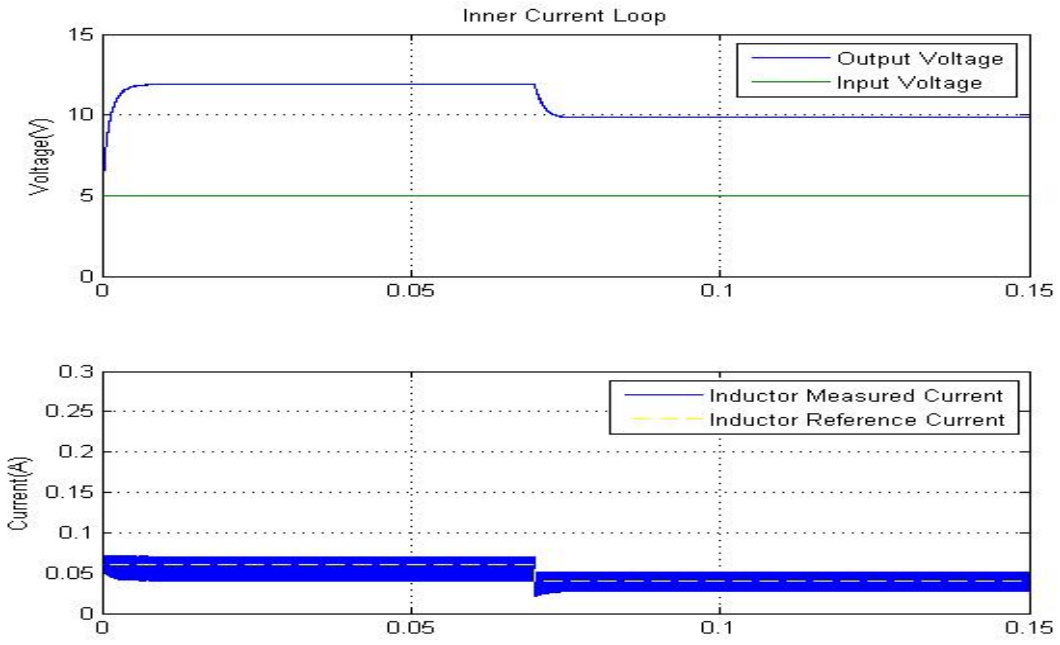

Figure 3.3: Inner Control Loop Plot

3.4.2 Simulations of Cascaded Control Structure

- **Step Change of Reference Voltage**

Considering Boost Converter parameters initially as V_{in} = 5V, L = 330mH, R = 820Ω and C = 4.7uF, while the reference voltage V_{REF} is changed from 9 V to 12 V at t=0.02sec. The output voltage and current transient response is shown in Figure 3.4.

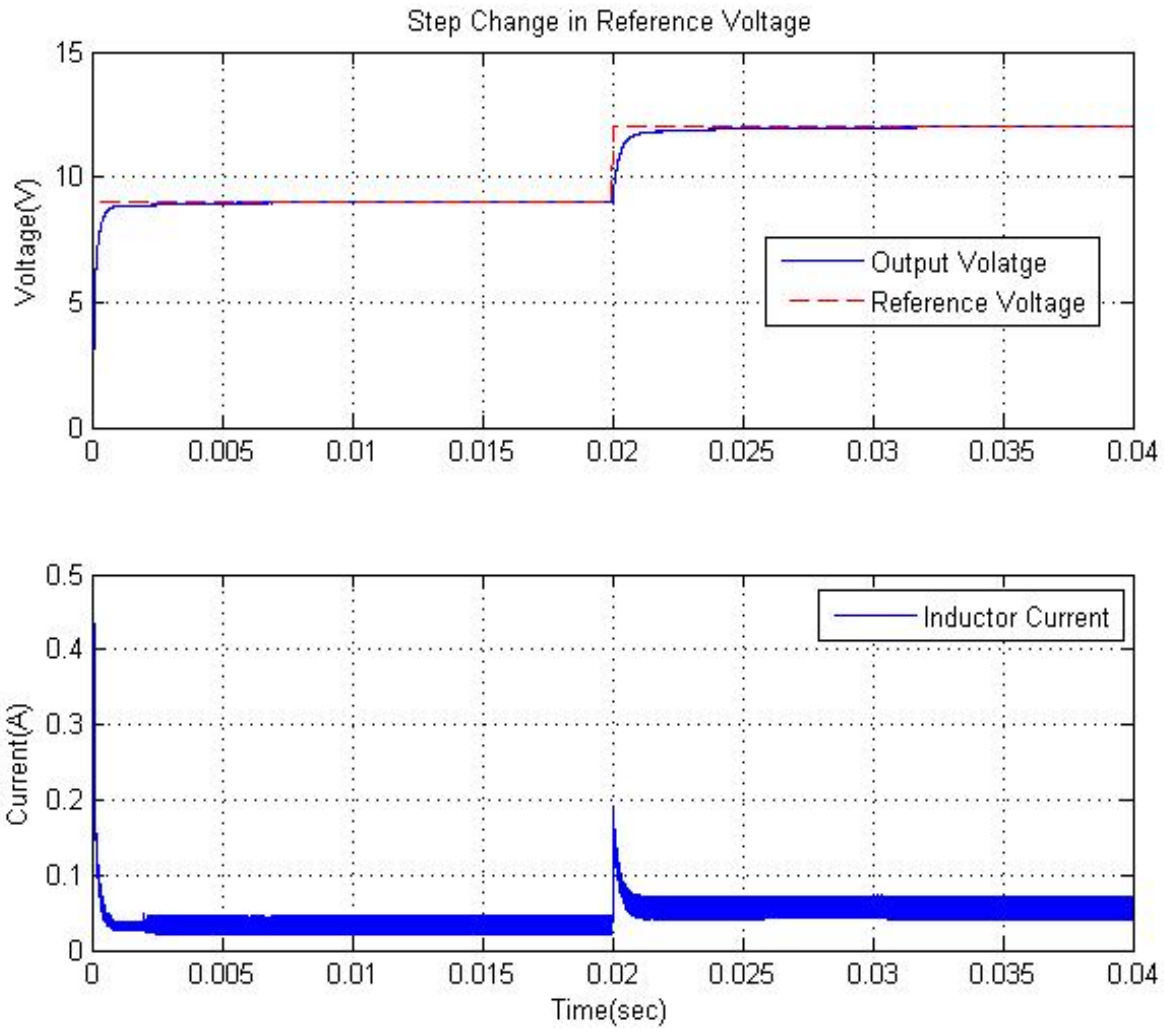

Figure 3.4: Step Change Of Reference Voltage

It is evident from simulation results as shown in Figure 3.4 that input voltage tracks the reference voltage. At time 0.02s, when reference voltage is changed, the controller

remains stable and insensitive to this parametric change. Inductor current goes in opposite direction at 0.02sec and gets stable again because the system is non-minimum phase.

- **Step Change of Input Voltage**

Considering DC/DC Boost Converter parameters initially as V_{REF} = 12V, L = 330mH, R = 820Ω and C = 4.7uF, while the input voltage V_{in} is decreased from 5 V to 3 V at t=0.02sec. The output voltage and current transient response is shown in Figure 3.5.

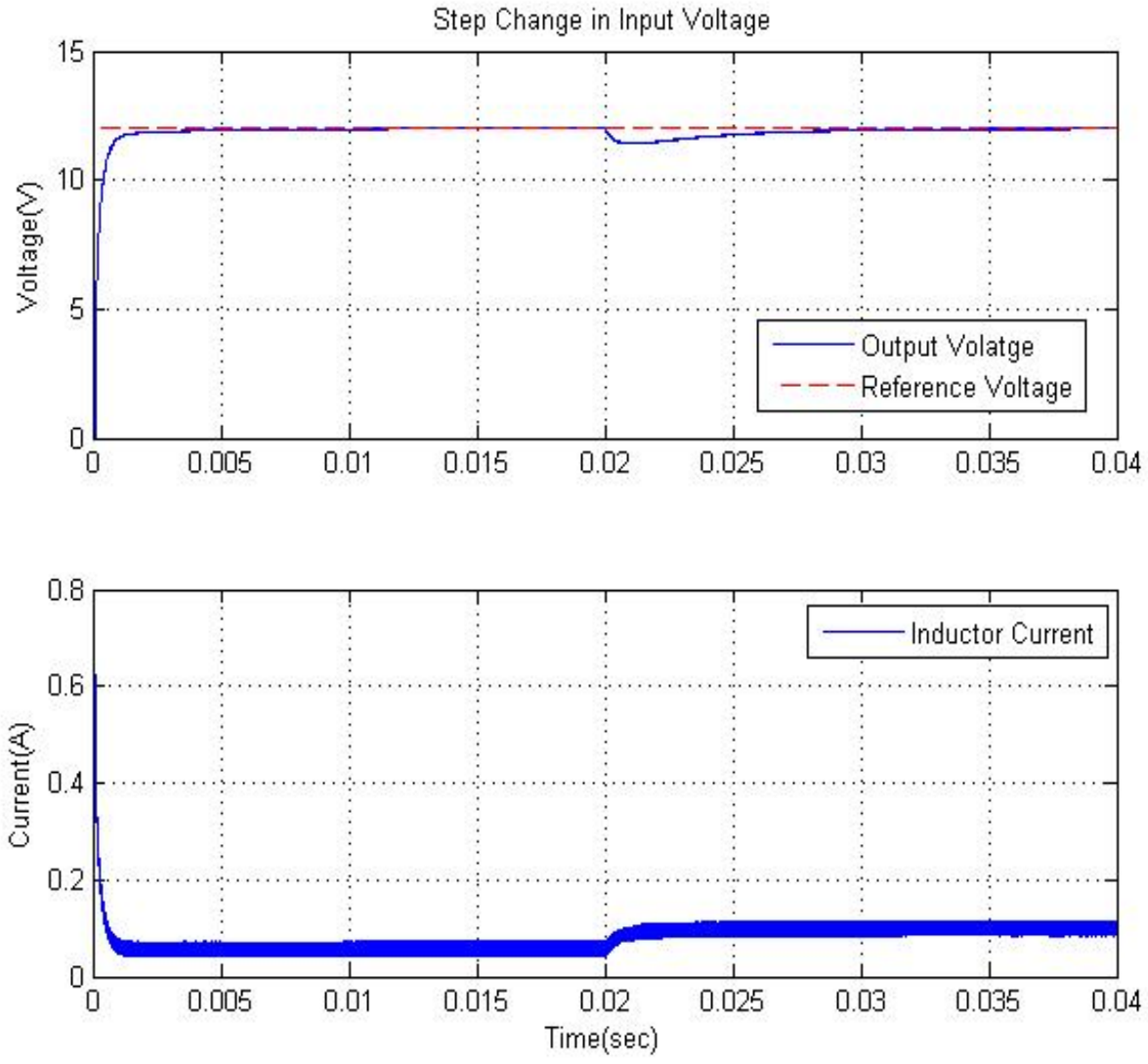

Figure 3.5: Step Change in Input Voltage

It can be seen in simulation results in Figure 3.4 that input voltage tracks the reference voltage. At time 0.02s, when input voltage is decreased, the controller remains stable and insensitive to this parametric change.

- **Step Change of Load Resistance**

Considering DC/DC boost converter parameters initially as V_{in} = 5V, V_{REF} = 12V ,L = 330mH and C = 4.7uF, while the load resistance R is changed from 820Ω to 410Ω at t=0.02sec. The output voltage and current transient response is shown in Figure 3.6.

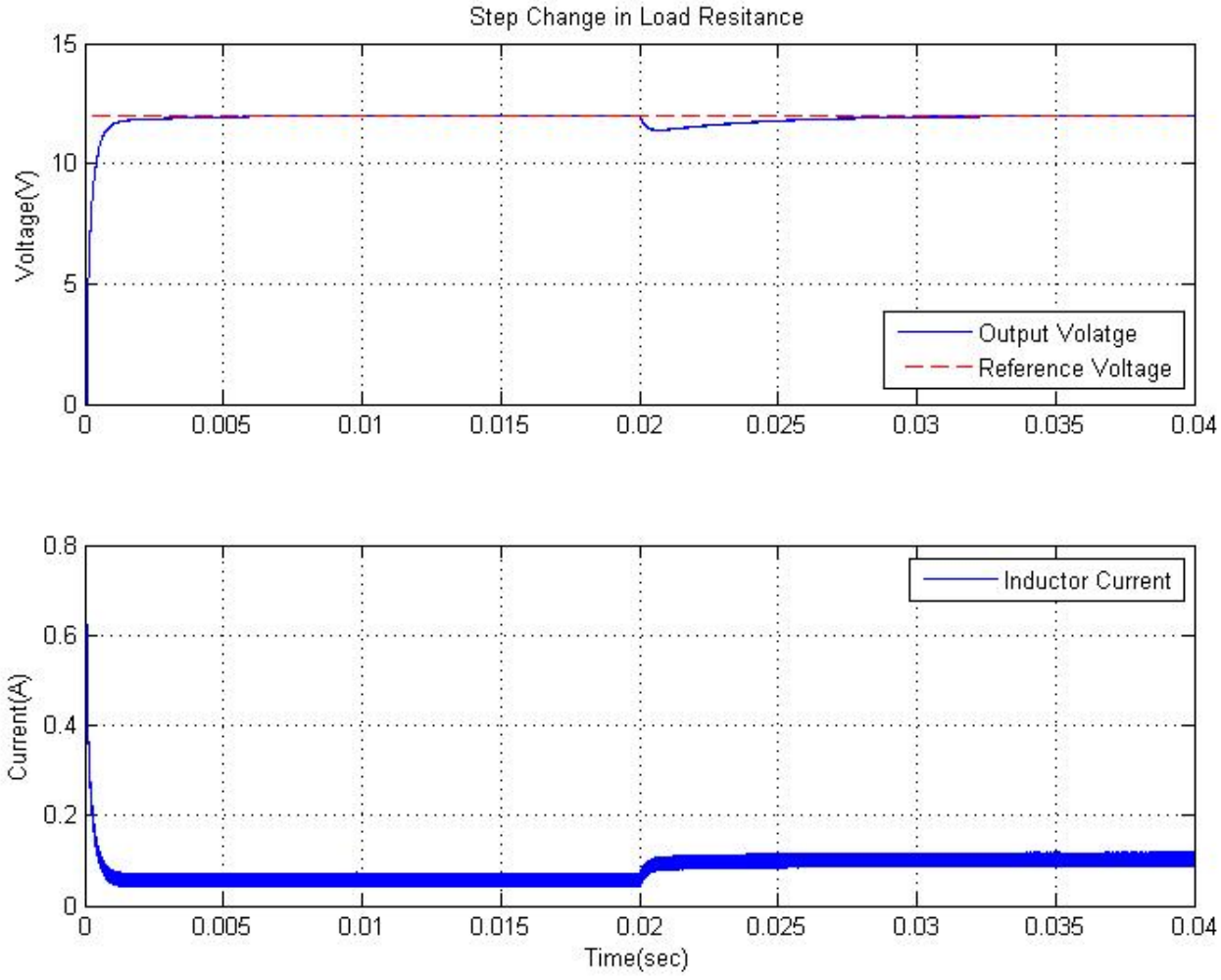

Figure 3.6: Step Change In Load Resistance

It can be seen in simulation results in Figure 3.4 that input voltage tracks the reference voltage. At time 0.02s, when input voltage is decreased, the controller remains stable and insensitive to this parametric change.

3.5 Conclusion

In this chapter, we have briefly discussed the control techniques that can be used to control the DC/DC Boost Converter. The Current-Mode control technique is opted because of its fast response to parametric variations. Due to its cascaded structure, inner and outer discussed separately and their controllers are designed respectively. The stability analysis of the Sliding Mode Controller is also shown. Simulations are performed and results are incorporated to ensure the robustness of the controller against system's unmodeled perturbations and external disturbances.

Chapter 4 Sensor-less Control Design Technique

4.1 Introduction

Sensor-less control design technique itself elaborates that this technique is utilized when we want to avoid the usage of the sensor in our design. This technique is always considered a better cost effective alternative to the sensor. It also reduces the risk of miss-wiring because of reduction of hardware circuitry. It also increases re-configurability of the design. In this technique, the unknown state is measured on the basis of available output states and plant model itself.

The Current-Mode control design technique, mentioned in previous chapter, takes output voltage V_o and inductor current I_L as a feedback. In practical implementation, if output voltage is greater than Reference voltage of Analog to Digital Converter (ADC), voltage divider network can be used. However, current sensor would be required for measurement of inductor current I_L.

The inclusion of a current sensor would add cost to the design, which can be either high or low depending upon the measurement accuracy. The current sensor can be replaced with estimation algorithm which estimates the state I_L using state observer.

4.2 Typical State Observer

A typical state observer estimates the internal state of the system using the input and output measurements. It can be implemented digitally with controller on any embedded platform. Let's consider the linear time invariant system as

$$\dot{\boldsymbol{x}} = \boldsymbol{Ax} + \boldsymbol{Bu} \qquad (15)$$

$$\boldsymbol{y} = \boldsymbol{Cx} \qquad (16)$$

Where x is plant state, *u* is input and *y* is output.

The output *y* of the plant is capable to drive any state of the state observer, if the system *(A, C)* is observable. The observer equations for the system are

$$\hat{\boldsymbol{x}} = \boldsymbol{A}\hat{\boldsymbol{x}} + \boldsymbol{Bu} \quad (\mathbf{17})$$

$$\hat{\boldsymbol{y}} = \boldsymbol{C}\hat{\boldsymbol{x}} \quad (\mathbf{18})$$

Where $\hat{\boldsymbol{x}}$ is plant observed state, *u* is input and $\hat{\boldsymbol{y}}$ is observed output state. Since the model is non-linear, the observers designed for the plant model are

- Sliding Mode Observer
- High Gain Observer

4.3 Sliding Mode Observer

Variations of parameters such as load, input voltage etc, are common in DC/DC converters. Classical Observers are not capable to obtain the unknown states of the system due to its non-linear behavior. The Sliding Mode Observer is one of the techniques that is usually adapted to find out the unknown states of such systems.

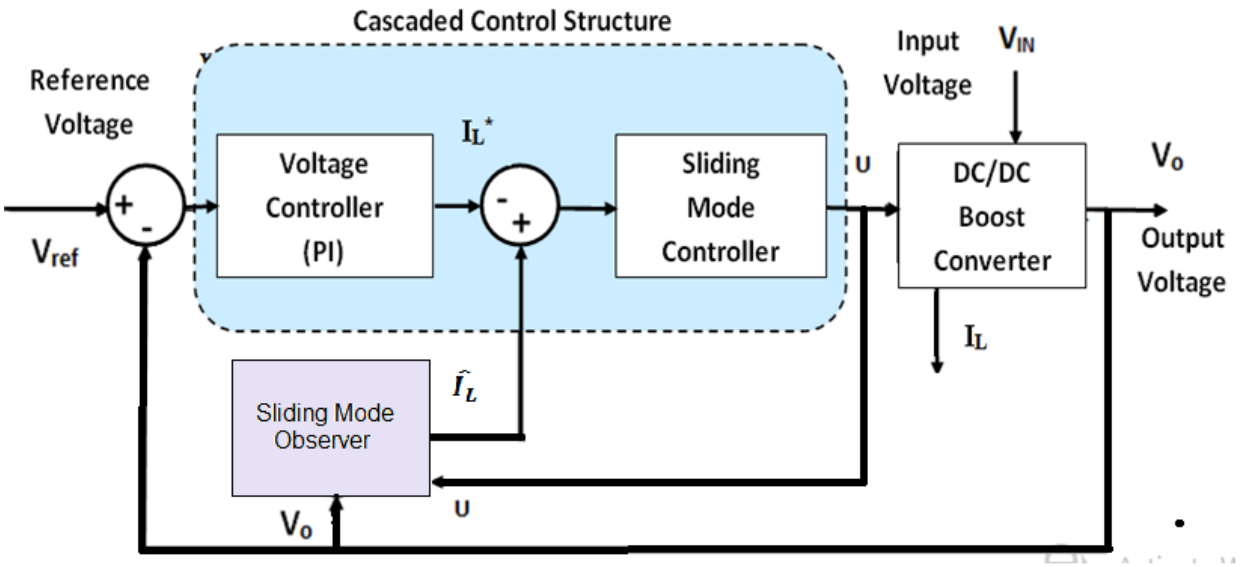

Figure 4.1: Sliding Mode Observer In DC/DC Boost Converter

The Sliding Mode Observer estimates the unknown states that cannot be measured directly. The observer model comprises of the state space model of the system for the estimation of the Inductor Current (the unknown state) and Capacitor Voltage [16]. The state estimation also requires the Output voltage V_o as a feedback and input voltage V_{in} as shown in Figure 4.1.

4.3.1 Design of Sliding Mode Observer

As mentioned in equation (7), the state space model for DC/DC Boost Converter is,

$$\dot{\mathbf{x}} = \mathbf{Ax} + \mathbf{Bu}$$

$$\dot{x} = \begin{bmatrix} 0 & -\frac{(1-u)}{L} \\ \frac{(1-u)}{C} & -\frac{1}{RC} \end{bmatrix} \begin{bmatrix} x_1 \\ x_2 \end{bmatrix} + \begin{bmatrix} \frac{1}{L} \\ 0 \end{bmatrix} V_{in}$$

where $x_1 = \mathbf{I_L}$ and $x_2 = \mathbf{V_o}$, $x = [x_1\ x_2]^T$, and control **u** has two possible discrete values (**0 or 1).** So,

$$\dot{I}_L = -\frac{(1-u)V_o}{L} + \frac{V_{in}}{L}$$

$$\dot{V}_o = \frac{(1-u)I_L}{C} - \frac{V_O}{R*C}$$

The Observer equation for above mentioned plant model is obtained by adding a non-linear gain which is proportional to the signum of the difference between measured output and observed value [16].

$$\dot{\hat{x}} = A\hat{x} + Bu + l * sign\,(y - C\hat{x})$$

$$\dot{\widehat{\mathrm{I}_{\mathrm{L}}}} = -\frac{(1-u)\widehat{V_o}}{L} + \frac{V_{in}}{L} + +l_1 * sign\,(y - C\hat{x}) \tag{19}$$

$$\dot{\widehat{\mathrm{V}_{\mathrm{o}}}} = \frac{(1-u)\widehat{I_L}}{C} - \frac{\widehat{V_O}}{R*C} + +l_2 * sign\,(y - C\hat{x}) \tag{20}$$

Where y = Vo and C$\hat{x}$ = $\widehat{Vo}$, and $\widetilde{V_o} = \widehat{V_o} - V_o$

Here, we want to design the sliding mode observer gain $\boldsymbol{l} = [\boldsymbol{l_1}\ \boldsymbol{l_2}]^{\boldsymbol{T}}$ such that the observer converges to hyper surface in finite time i.e. $\mathbf{lim_{t\to\infty}}\,\tilde{\mathbf{x}}\,(\mathbf{t}) = \mathbf{0}$, where $\tilde{x}$ is the error between measured and observed states [16]. Hence,

$$\tilde{x} = \hat{x} - x = 0 \tag{21}$$

When the error $\tilde{x}$ = 0, the rate of change of the error will also be zero. Hence,

$$\dot{\tilde{x}} = \dot{\hat{x}} - \dot{x} = 0 \tag{22}$$

Where, = $[x_1\ x_2]^T$, x_1= $\mathbf{I_L}$ and x_2 = $\mathbf{V_o}$.

So, we can write the Observer error equations as,

$$\dot{\widetilde{I_L}} = \frac{-(1-u)\widetilde{V_o}}{L} + l_1 * sign\left(\widetilde{V_o}\right) \tag{23}$$

$$\dot{\widetilde{V_O}} = \frac{(1-u)\tilde{I_L}}{C} - \frac{\widetilde{V_o}}{RC} + l_2 * sign\left(\widetilde{V_o}\right) \tag{24}$$

As mentioned in equation (21) and (22), by putting $\tilde{I_L} = \dot{\tilde{I}}_L = \dot{\tilde{V}}_o = 0$ in equation (23) and (24) ,the observer gain equations are determined as,

$$l_1 = -k_1 * \frac{(1-u)*\widetilde{V_o}}{L} \tag{25}$$

$$l_2 = k_2 * \frac{\widetilde{V_O}}{RC} \tag{26}$$

Where k_1 and k_2 are used to improve transient response of the observer.

4.3.2 Simulation Results of Sliding Mode Observer

- **Step change in Load Resistance**

Considering DC/DC boost converter parameters initially as V_{in} = 5V, V_{ref} = 12V, L = 330mH and C = 4.7uF, Load resistance R changes from 820Ω to 410Ω at 0.07s. Simulation is performed to verify the estimation of the inductor current using the Sliding Mode Observer. Figure 4.4 shows the tracking of output voltage with respect to the reference voltage.

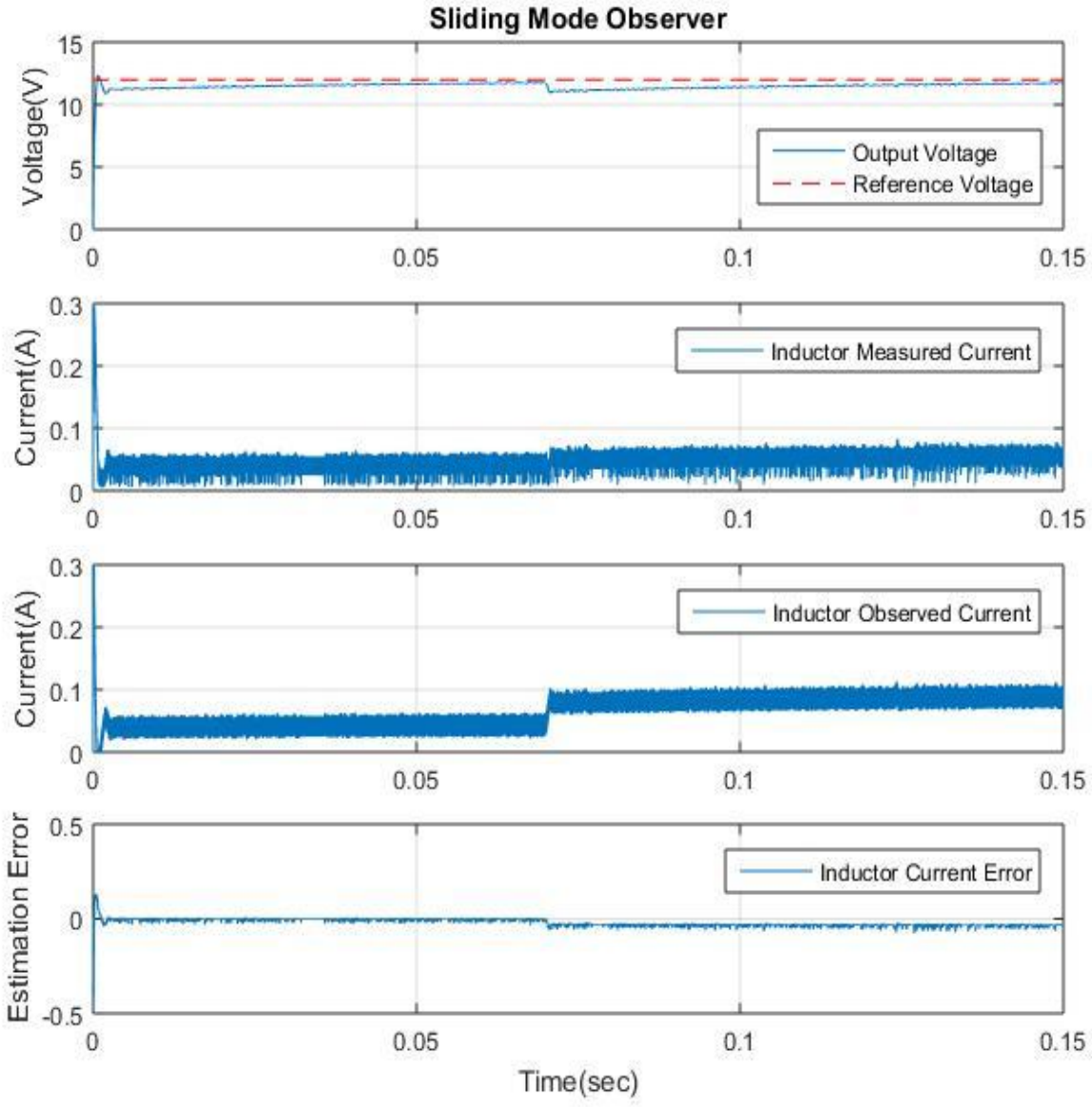

Figure 4.2: Sliding Mode Observer Estimation Plot for Load Variation

- **Step Change in Input Voltage**

Considering DC/DC boost converter parameters initially as R = 820Ω, V_{ref} = 12V, L = 330mH and C = 4.7uF, Input voltage V_{in} changes from 5V to 3V at 0.07s. Simulation is performed to verify the estimation of the inductor current using the Sliding Mode Observer. Figure 4.3 shows the tracking of output voltage with respect to the reference voltage in the presence of parametric change of input voltage.

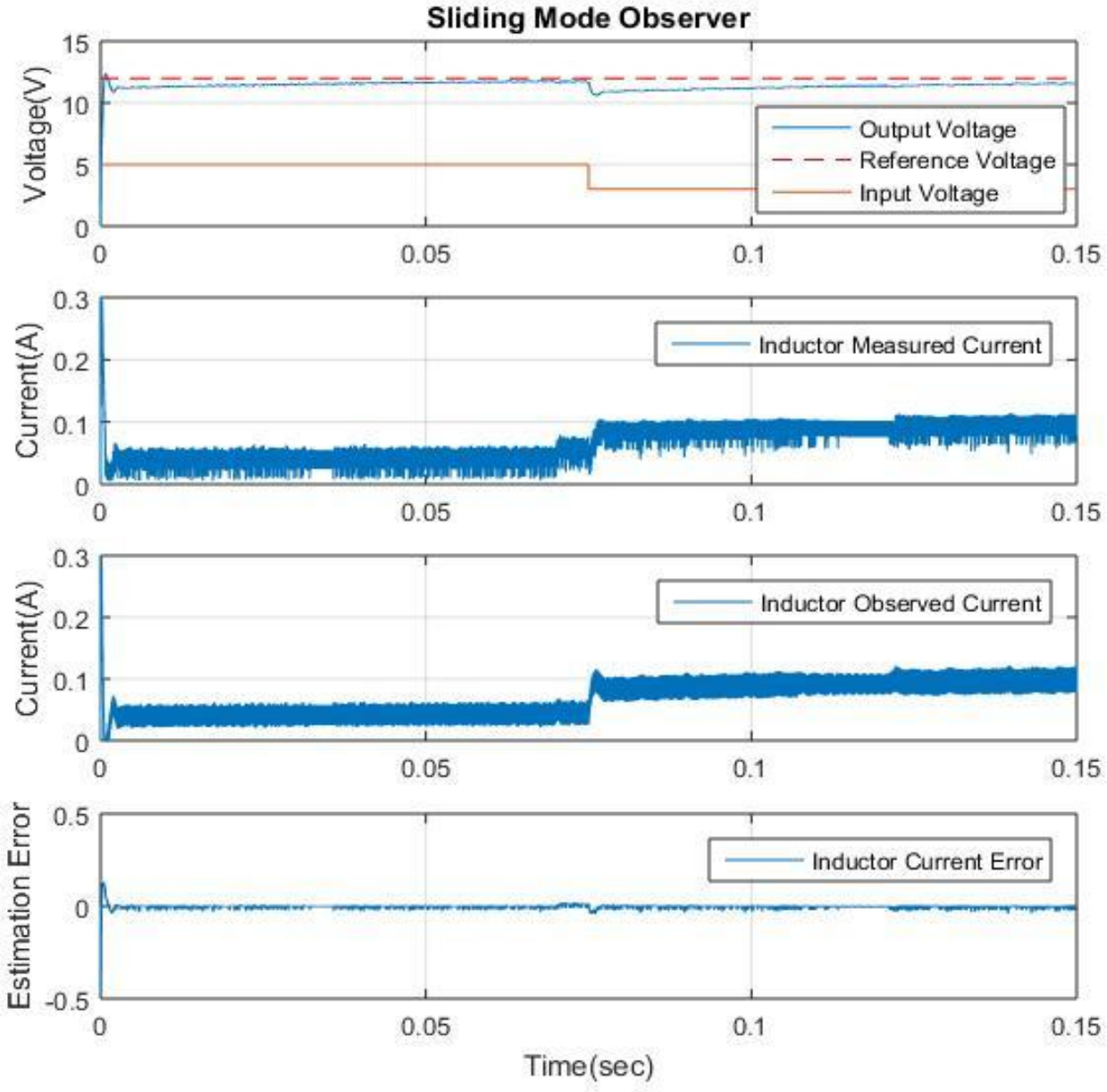

Figure 4.3: Sliding Mode Observer Estimation Plot for Input Voltage change

- **Step Change in Reference Voltage**

Considering DC/DC boost converter parameters initially as R = 820Ω, V_{in} = 5V, L = 330mH and C = 4.7uF, Reference voltage V_{ref} = 12V changes from 12V to 9V at 0.07s. Simulation is performed to verify the estimation of the inductor current using the Sliding Mode Observer. Figure 4.4 shows the tracking of output voltage with respect to the reference voltage which changes in real time.

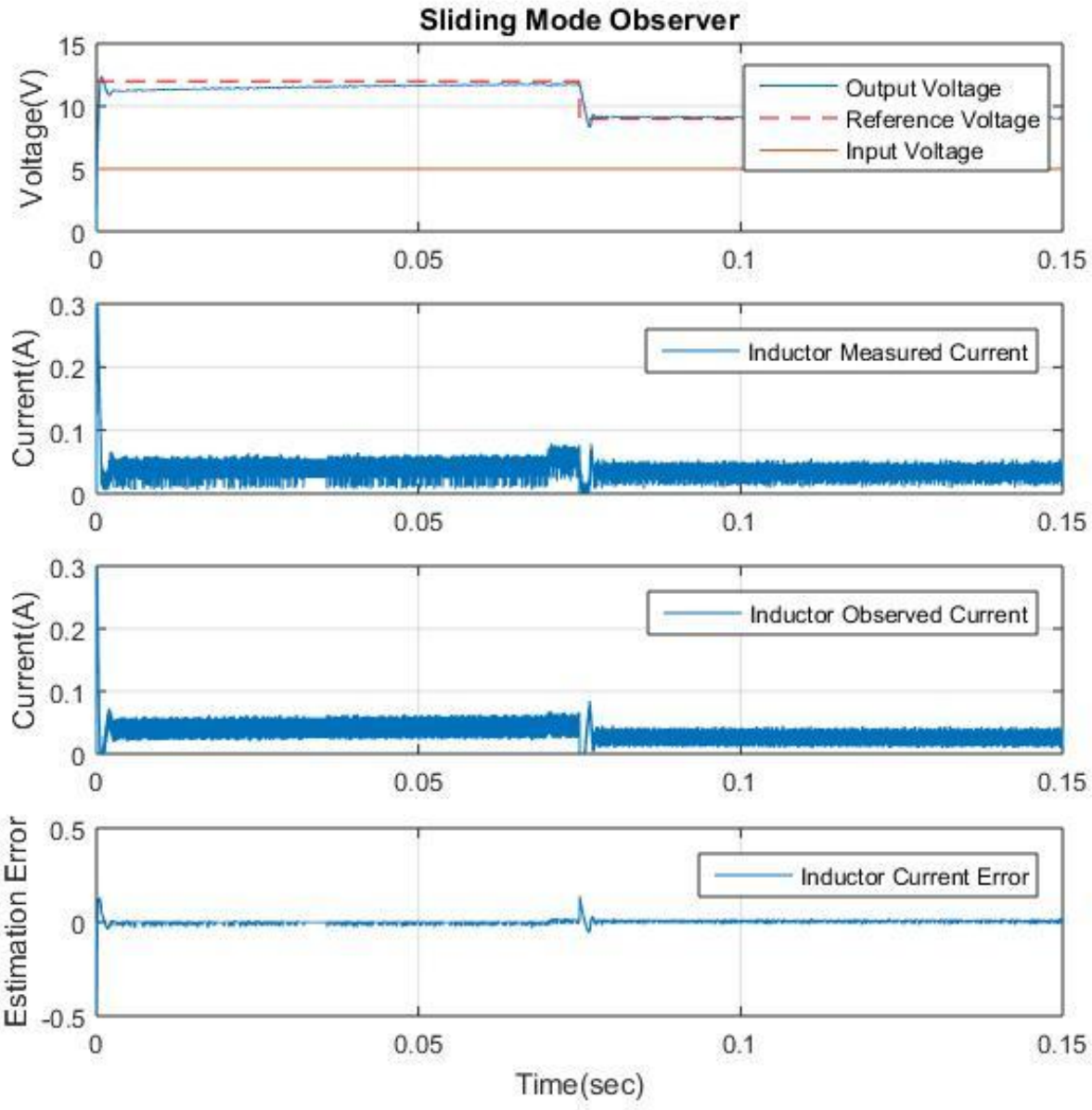

Figure 4.4: Sliding Mode Observer Estimation Plot for Reference Voltage change

Simulation results in Figure 4.2, Figure 4.3 and Figure 4.4 show three different scenarios regarding parametric variations. It clearly shows in these results that the observed current $\widehat{I_L}$ which is acquired by the estimation algorithm is following the same path of the measured current I_L regardless of parametric variations. The estimation error $\tilde{I}_L$ is shown in order to prove the accuracy of the Sliding Mode Observer to estimate the inductor current which remains insensitive to change in reference voltage, input voltage and load in real time. This shows that Sliding Mode Observer remains stable in all the above mentioned testing scenarios.

Hence selection of the gains k_1 and k_2 is done in such a way that transient response can be improved. DC/DC Boost Converter output voltage achieves the steady state by approaching the reference voltage in 50ms as shown in Figure 4.2.

4.4 High Gain Observer

High Gain Observer estimates the unknown state of the system that cannot be measured directly in DC/DC Boost Converters. It is robust enough to estimate state of the non-linear system in the presence of uncertainties. It follows the required trajectory to estimate the unknown desired state without the help of switching functions, unlike Sliding Mode Observer which results in chattering. Chattering causes more heat dissipation and it also reduces accuracy of the observed value[20].

In our design, the inductor current and output voltage are estimated using High Gain Observers. The inductor current is the required unknown state for Sliding Mode Controller. Therefore, both Sliding Mode Control as output feedback control and High Gain Observer as state feedback control, are working on *Separation Principle* [20].

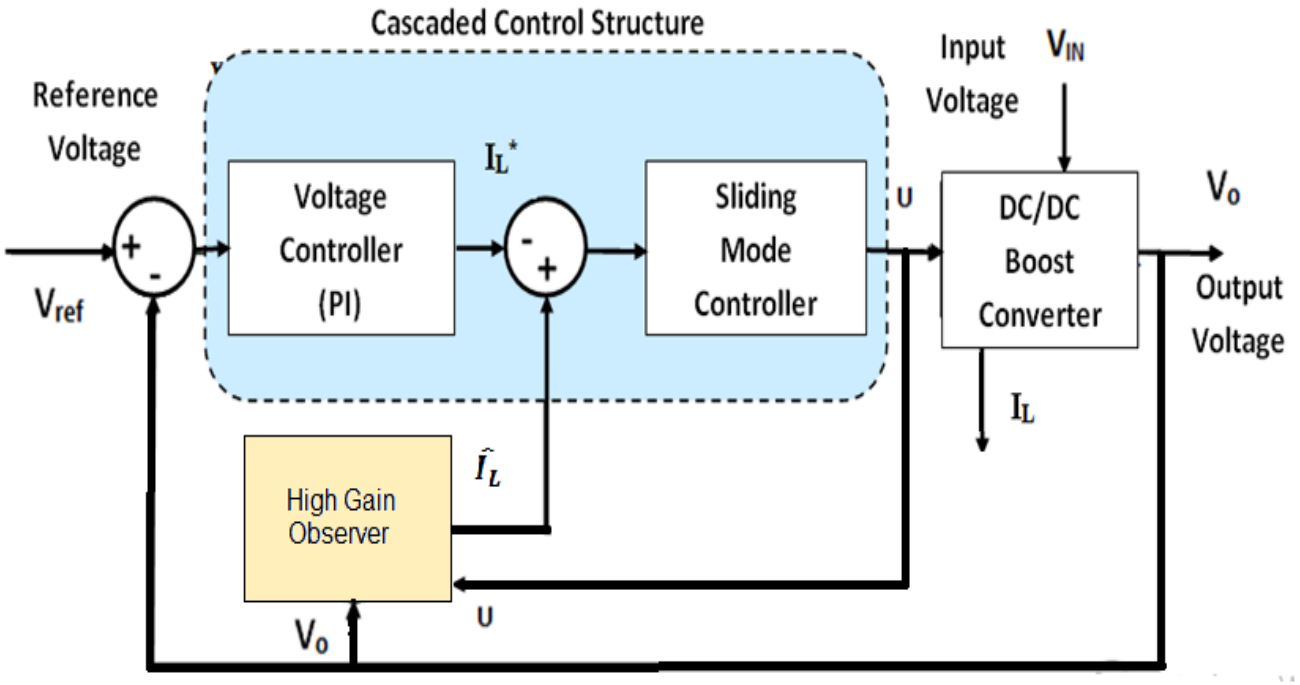

Figure 4.5: High Gain Observer in Boost Converter

4.4.1 Design of High Gain Observer

As mentioned in equation (7), the state space model for DC/DC Boost Converter is

$$\dot{\mathbf{x}} = \mathbf{Ax} + \mathbf{Bu}$$

$$\dot{x} = \begin{bmatrix} 0 & -\frac{(1-u)}{L} \\ \frac{(1-u)}{C} & -\frac{1}{RC} \end{bmatrix} \begin{bmatrix} x_1 \\ x_2 \end{bmatrix} + \begin{bmatrix} \frac{1}{L} \\ 0 \end{bmatrix} V_{in}$$

where x_1= $\mathbf{I_L}$ and x_2 = $\mathbf{V_o}$, $x = [x_1\ x_2]^T$, *a*nd control **u** has two possible discrete values (**0 or 1).**

$$\dot{\mathrm{I}}_{\mathrm{L}} = -\frac{(1-u)V_o}{L} + \frac{V_{in}}{L}$$

$$\dot{\mathrm{V}}_{\mathrm{o}} = \frac{(1-u)I_L}{C} - \frac{V_O}{R*C}$$

The observer equation for above mentioned plant model is obtained by adding a non-linear high gain which is proportional to the difference between measured output and observed value.

$$\dot{\hat{x}} = A\hat{x} + g(y,u) + H*(y - C\hat{x}) \tag{27}$$

The estimation error $\tilde{x} = \hat{x} - x$ must satisfy the linear equation,

$$\dot{\tilde{x}} = (\mathrm{A} - \mathrm{HC}) * \tilde{x} \tag{28}$$

Asymptotic error convergence $\mathbf{lim_{t\to\infty}\,\tilde{x}\,(t) = 0}$ can be guaranteed by designing C to make **A - HC** Hurwitz.

High Gain Observer equation for the DC/DC Boost Converter can be written as,

$$\dot{\widehat{\mathrm{I}}}_{\mathrm{L}} = -\frac{(1-u)\widehat{V_o}}{L} + \frac{V_{in}}{L} + +h_1 * (y - C\hat{x}) \tag{29}$$

$$\dot{\widehat{\mathrm{V}}}_{\mathrm{o}} = \frac{(1-u)\widehat{I_L}}{C} - \frac{\widehat{V_O}}{R*C} + +h_2 * (y - C\hat{x}) \tag{30}$$

Where, $x = [I_L\ V_O]^T$, $x_1 = \boldsymbol{I_L}$ and $y = x_2 = \boldsymbol{V_O}$.

When the error $\tilde{x}$ = 0, the rate of change of the error will also be zero. Hence,

$$\dot{\tilde{x}} = \dot{\hat{x}} - \dot{x} = 0 \tag{31}$$

$$\dot{\tilde{x}} = \begin{bmatrix} \dot{\tilde{I}}_L \\ \dot{\tilde{V}}_O \end{bmatrix} = \begin{bmatrix} \dot{\hat{I}}_L - \dot{I}_L \\ \dot{\hat{V}}_O - \dot{V}_O \end{bmatrix} = 0 \tag{32}$$

So, we can write the Observer error equations as,

$$\dot{\tilde{I}}_L = \frac{-(1-u)\tilde{V}_o}{L} + h_1 * (\tilde{V}_o) \tag{33}$$

$$\dot{\tilde{V}}_O = \frac{(1-u)\tilde{I}_L}{C} - \frac{\tilde{V}_o}{RC} + h_2 * (\tilde{V}_o) \tag{34}$$

The Observer gains can be tuned as follows,

$$h_1 = {}^{\alpha_1}/_{\varepsilon} \tag{35}$$

$$h_2 = {}^{\alpha_2}/_{\varepsilon^2} \tag{36}$$

Such that $h_2 \gg h_1 \gg 1$.

Where α_1 , α_2 and ε are positive constants with $\varepsilon \ll 1$ as mentioned in [20].

4.4.2 Simulation Results of High Gain Observer

- **Step Change in Load Resistance**

Considering DC/DC boost converter parameters initially as V_{in} = 5V, V_{ref} = 12V, L = 330mH and C = 4.7uF, Load resistance R changes from 820Ω to 410Ω at 0.07s. Simulation is performed to verify the estimation of the inductor current using the High Gain Observer. Figure 4.4 shows the tracking of output voltage with respect to the reference voltage in the presence of load variation and it can be seen from figures that system remains stable under variation of load value in real time.

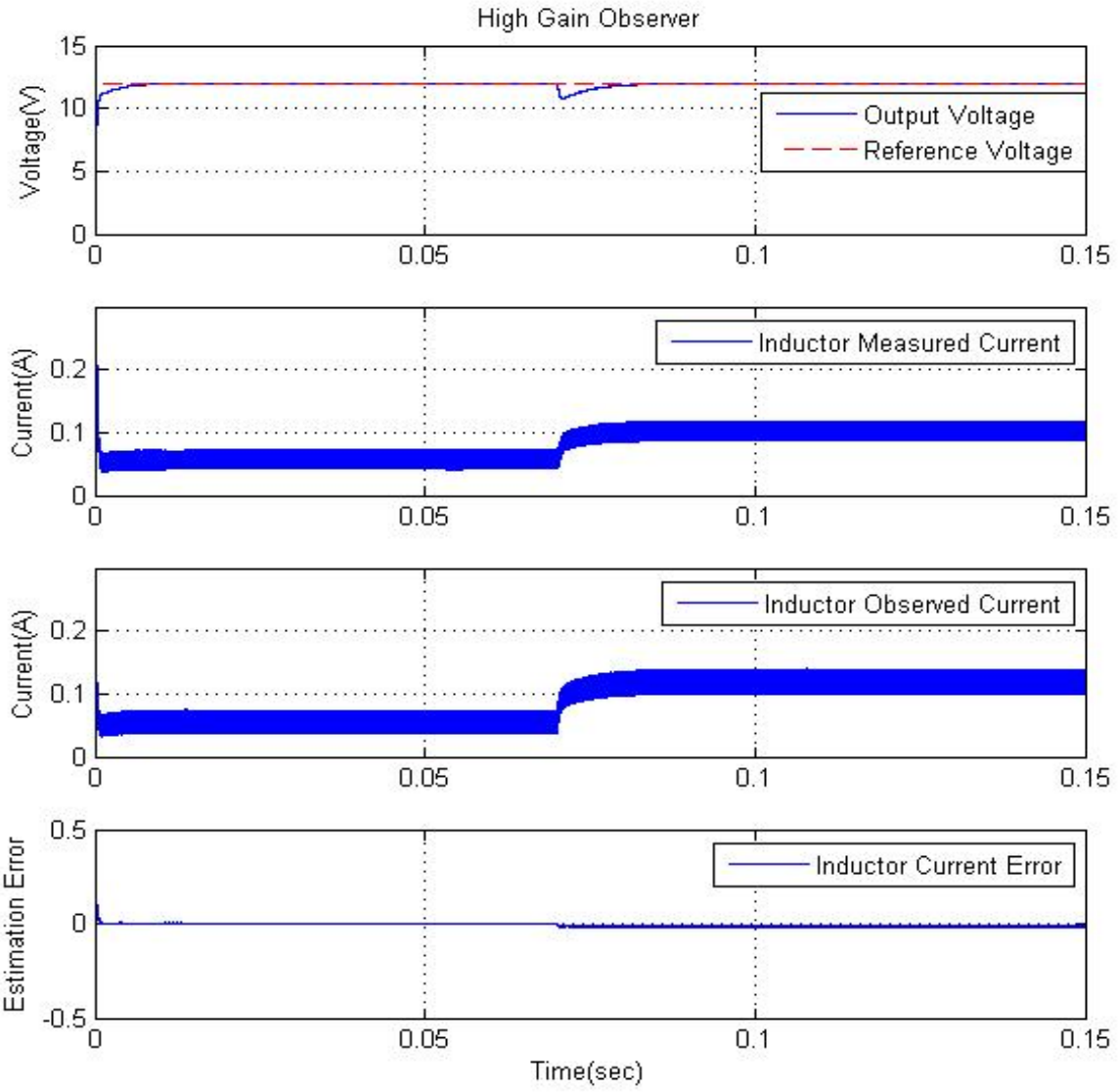

Figure 4.6: High Gain Observer Estimation Plot for Load Variation

- **Step Change in Input Voltage**

Considering DC/DC boost converter parameters initially as R = 820Ω, V_{ref} = 12V, L = 330mH and C = 4.7uF, Input voltage V_{in} changes from 5V to 3V at 0.07s. Simulation is performed to verify the estimation of the inductor current using the High Gain Observer. Figure 4.5 shows the tracking of output voltage with respect to the reference voltage in the presence of

parametric change of input voltage.

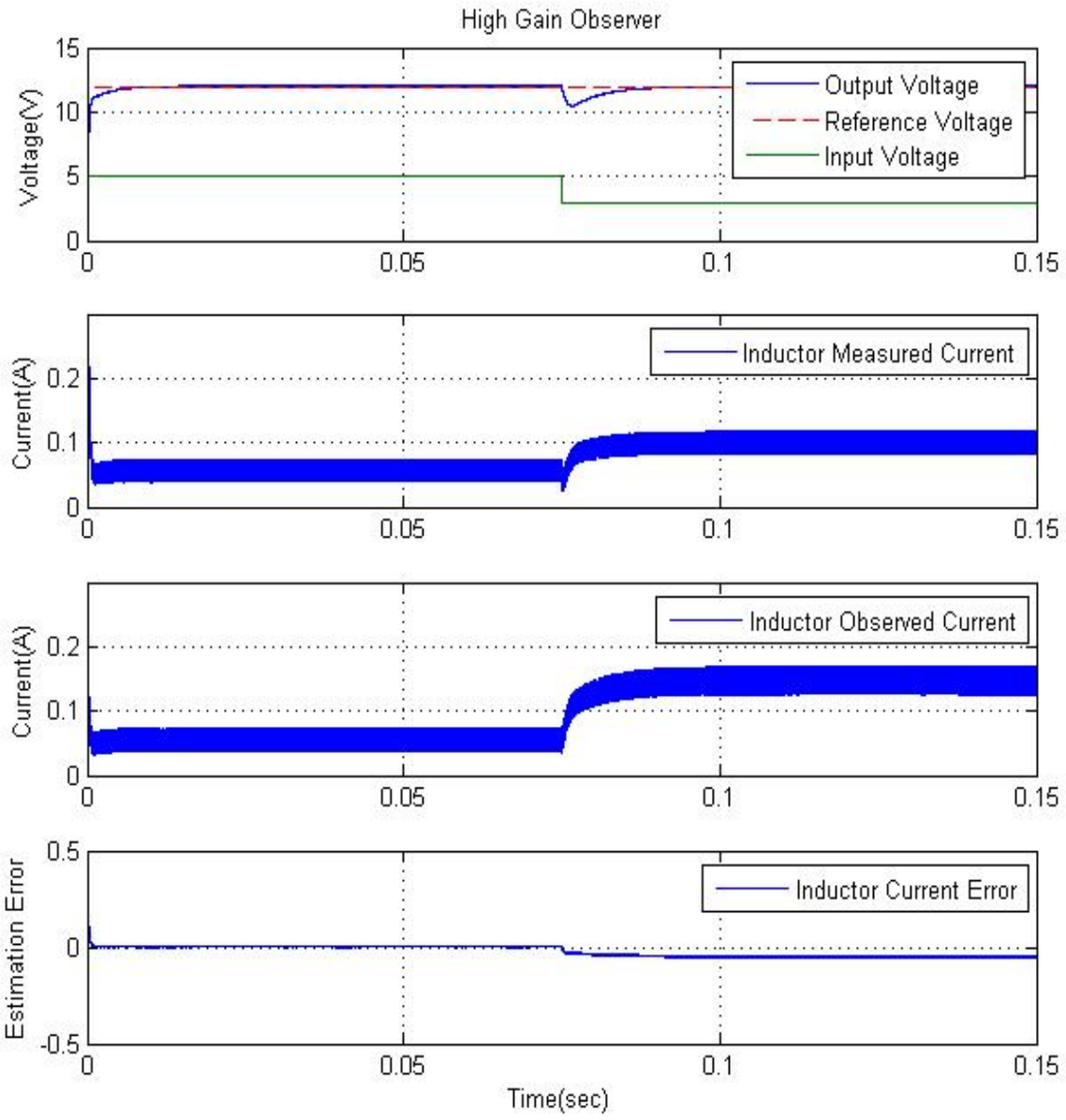

Figure 4.7: High Gain Observer Plot for input voltage variation

- **Step Change in Reference Voltage**

Considering DC/DC boost converter parameters initially as R = 820Ω, V_{in} = 5V, L = 330mH and C = 4.7uF, Reference voltage V_{ref} = 12V changes from 12V to 9V at 0.07s. Simulation is performed to verify the estimation of the inductor current using the High Gain

Observer. Figure 4.6 shows the tracking of output voltage with respect to the reference voltage which changes in real time.

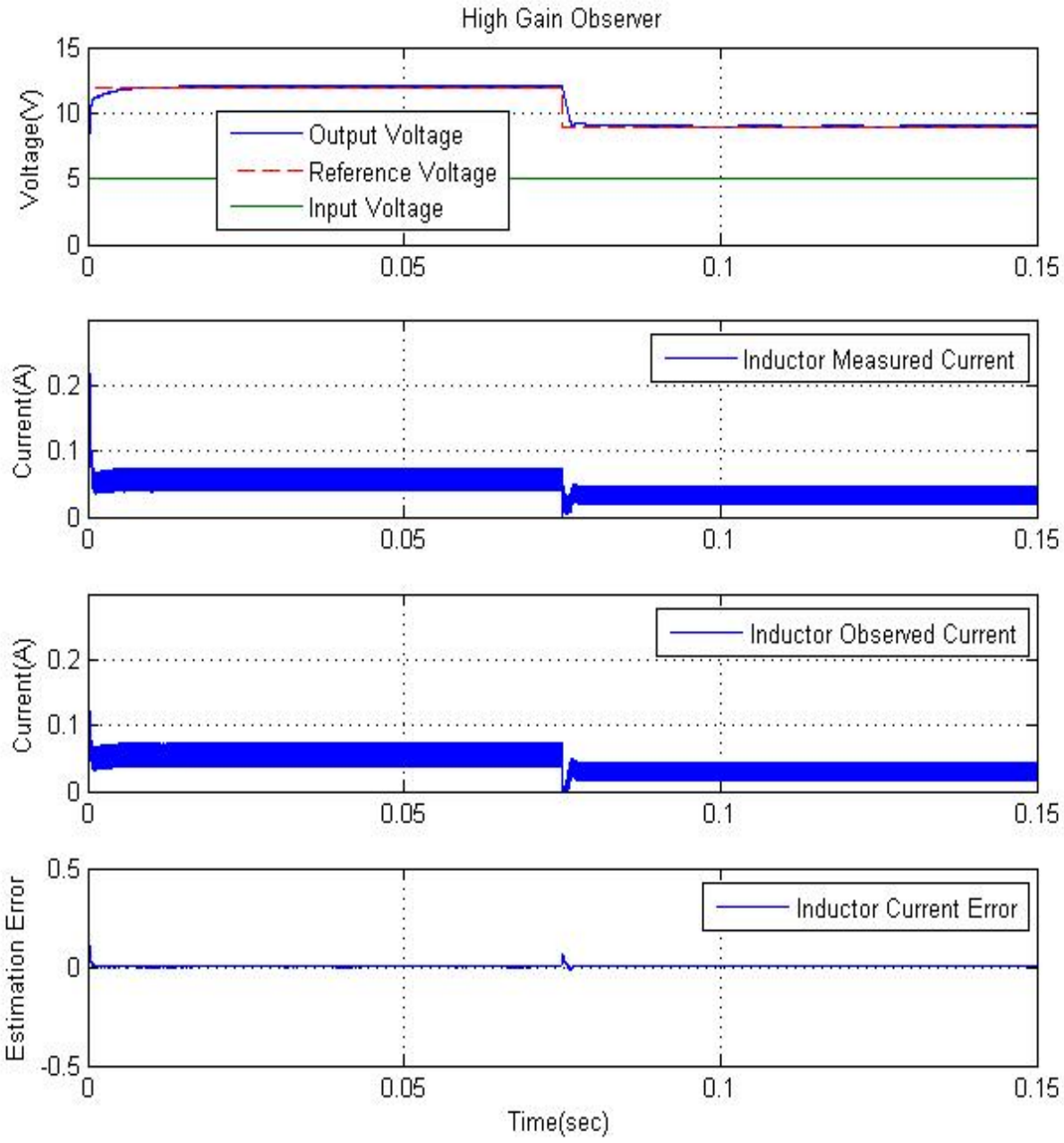

Figure 4.8: High Gain Observer Plot for reference voltage variation

Simulation results in Figure 4.6, Figure 4.7 and Figure 4.8 show three different scenarios regarding parametric variations. It clearly shows in these results that the observed current $\widehat{I_L}$ which is acquired by the estimation algorithm is following the same path of the measured current I_L regardless of parametric variations. The estimation error $\tilde{I}_L$ is shown in order to prove the accuracy of the High Gain Observer to estimate the inductor current which remains insensitive to change in reference voltage, input voltage and load in real time. This shows that High Gain Observer remains stable in all the above mentioned testing scenarios.

Hence, values of α_1, α_2 and ε are chosen to improve the transient response of the system. The output voltage of DC/DC Boost converter achieves steady state by approaching the reference voltage in 5ms and remains stable under load variation, input voltage and reference voltage variation in real time.

4.5 Conclusion

This chapter depicts the clear picture of the Sensor-less Control techniques used in the design. For this purpose, two kinds of observers are designed for the estimation of the unknown state i.e. inductor current. The observer algorithms behaved as the best alternatives for the actual sensors with the advantages and disadvantages. The equations for two algorithms, High Gain Observer and Sliding Mode Observer, are derived. Simulation results are presented, showing the steady state response in three different scenarios to verify the robustness of the non-linear observers.

Chapter 5 FPGA-IN-THE-LOOP Simulation

5.1 Introduction

The FIL (FPGA-IN-THE-LOOP) simulation provides the capability to test and verify a design at desired hardware speeds while using Simulink environment as a system level testbench. In FIL simulation, the data and parameters are passed to the FPGA device from MATLAB workspace and FPGA hardware results are read back in real time. FIL simulations are also useful in the case when controller implemented in FPGA is needed to be tested when real time plant is not available.

With the advancement in technology, the utilization of Field Programmable Gate Array (FPGA) devices is increasing. FPGA have large resources of gates and clock rates (up to 500 MHz) which allow designers to implement the complex computations and algorithms. Reconfigurability of FPGA provides designers flexibility to change or update their design in field as compared to the hard-wired circuits. Control Algorithms can fit into FPGAs rather than the microprocessors and digital signal processors (DSP) which has constraints of event sequencers and interrupts. Therefore, modern complex control algorithms can be easily implemented on FPGAs..Implementation of controllers on FPGA can boost their performance.

FPGAs provide dedicated hardware for implementation of logic unlike microprocessors having operating system. This enables multiple control designs to have separate hardware resources rather than competing for same processing sources. So, different algorithms and designs can run in parallel on same FPGA chip. It allows control algorithms to run on the same FPGA chip at different rates. In automobiles, there is a growing need of reducing the size of circuitry to implement Electronic Control Unit (ECU), Controller Area Network (CAN) controllers and other required units on the same FPGA chip. In that case, instead of using separate commercially available Integrated Circuits (ICs), the smart solution would be to implement it on the same FPGA chip.

5.2 FPGA Implementation using Xilinx System Generator

The Xilinx System Generator (XSG) tool enables the use of Simulink for implementing designs and complex algorithms on Xilinx FPGAs [9]. It is an easier way to implement DSP designs as compared to hardware description languages such as Verilog HDL and VHDL. Xilinx System Generator is used by the designers for fast prototyping of algorithms, if they want to implement in fast switching device such as FPGA.

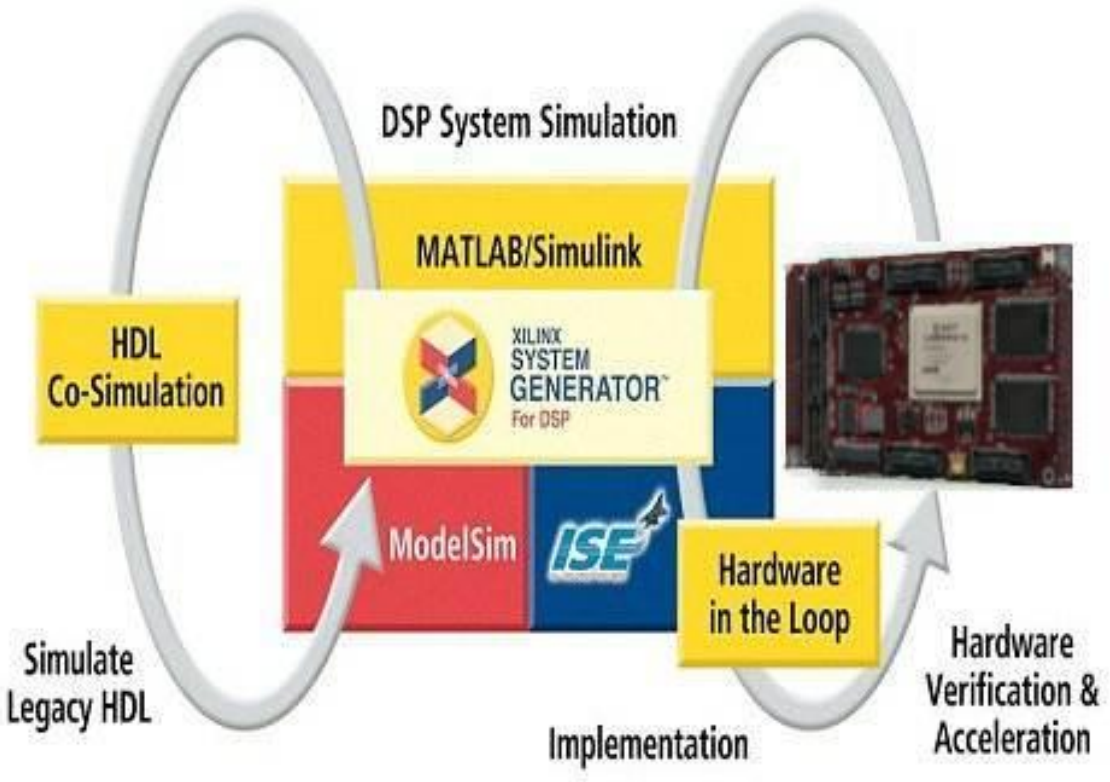

Figure 5.1: Xilinx System generator

Xilinx System Generator allows abstraction of complex algorithms through graphical modules and blocks provided by Simulink environment. Simulink contains library named as Xilinx-specific blocksets, which is a group of several primitive and digital signal processing functions. These functions allow prototyping of complex algorithms very easily using MATLAB/Simulink environment. Not only this, custom blocks can also be developed based on application requirements. Design flow of Xilinx System Generator is shown in figure 5.2

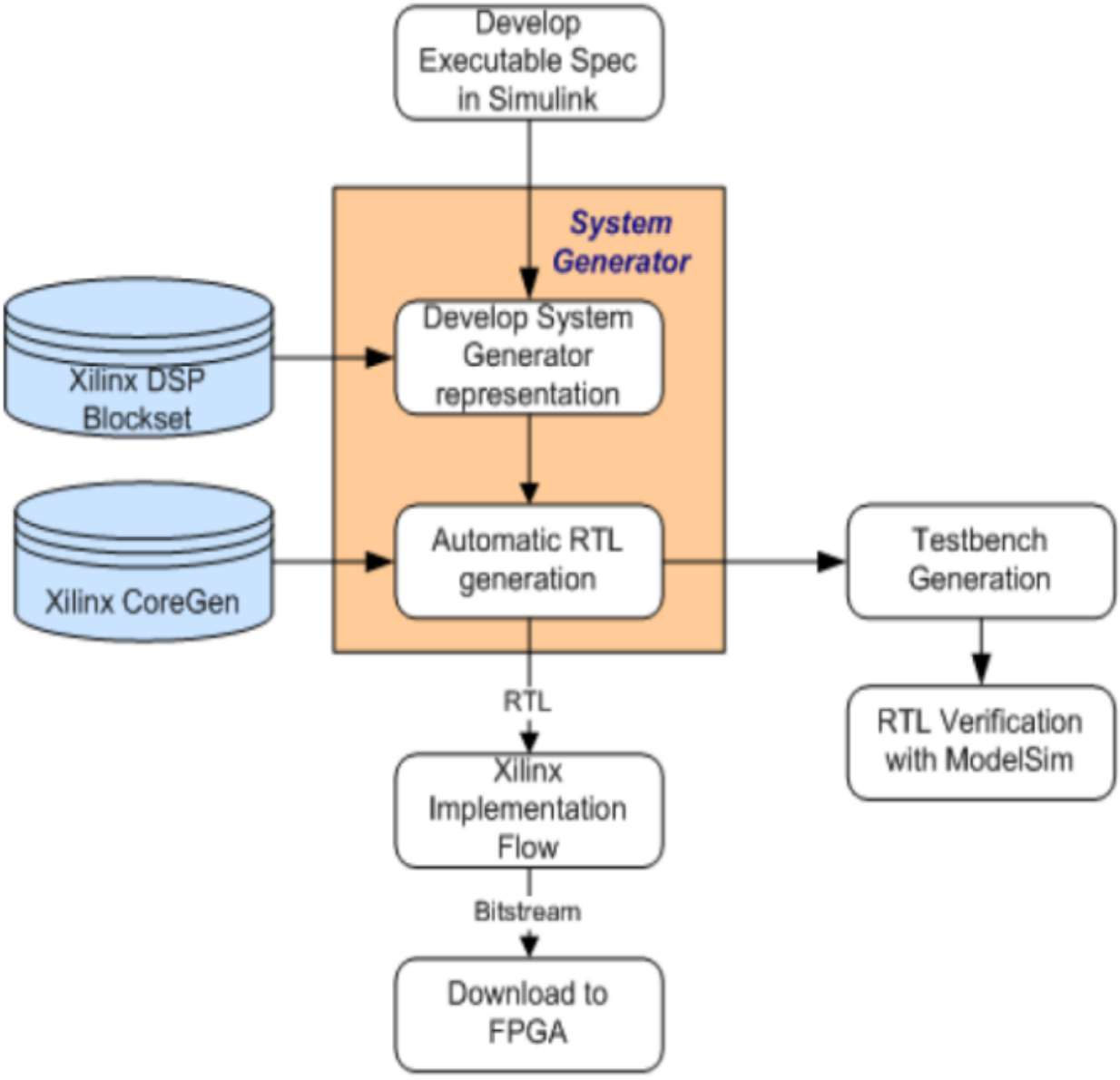

Figure 5.2: Design flow of Xilinx System Generator

The tool automatically converts the design into synthesizable HDL code, which is transformed to gate level netlist to be mapped on Xilinx FPGAs. It also generates HDL testbench to verify the design upon implementation. Another advantage is that we can perform HDL Co-simulation in which Simulink supported HDL simulators/verifiers such as Modelsim, Questa and Incisive etc are used to co-simulate design built through Xilinx blocks. During co-simulation, we can watch the waveforms of inputs, outputs and internal registers of the design.

Xilinx System Generator also enables users to verify their algorithms directly on hardware while using Simulink as their testbench using Hardware Co-Simulation. It automatically generates bitstream, associates it into a block and loads into targeted FPGA during compilation. This, in turn speeds up the simulation because design under test is running on dedicated hardware.

5.3 Brief Introduction of Target FPGA

The FPGA kit opted for implementation of the control design is Nexys4 DDR. This digital circuit development platform is based on latest Xilinx variant FPGA chip Artix7 (Xilinx part number XC7A100T-1CSG324C). Artix7 belongs to the latest 7 series of Xilinx products and is among the least cost variants of Xilinx FPGAs. It provides high performance and more resources as compared to earlier variants. Due to millions of logic elements, operating speeds exceeding 450MHz, dedicated DSP blocks, block rams, on-chip ADC (xADC) and the I/O peripheral support, this FPGA can be used in wide range of applications [21].

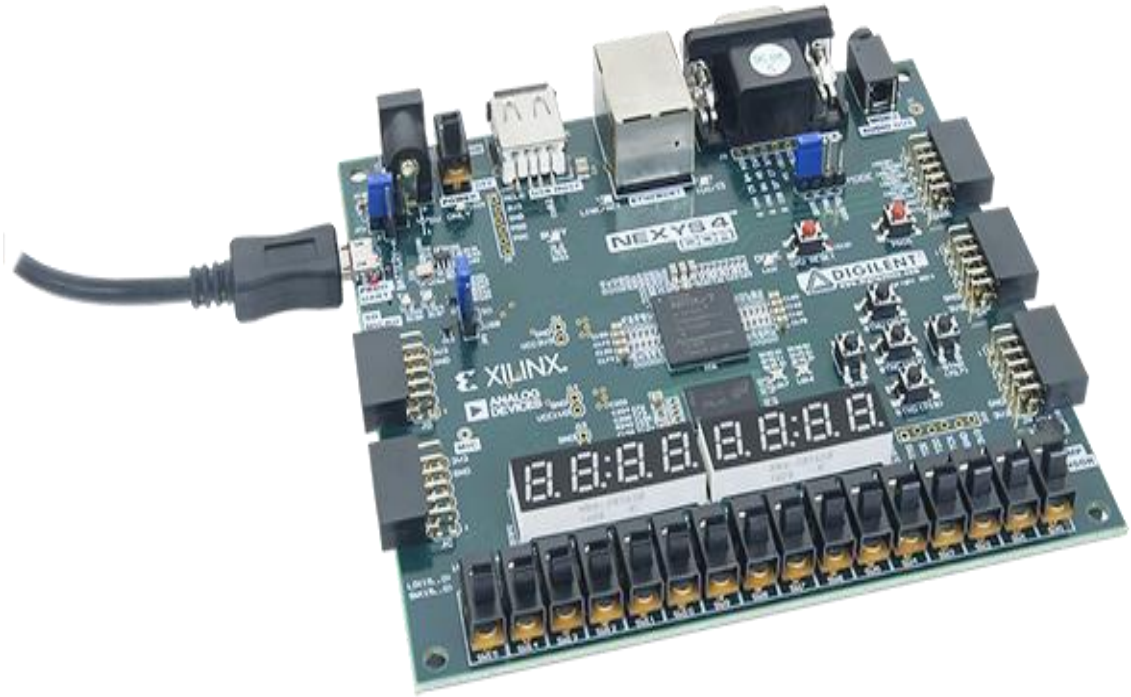

Figure 5.3: Nexys 4 DDR (ARTIX 7)

5.4 Implementation Methodology

As the control design is having complex equations, the floating point format is used for arithmetic operations and computations for accuracy and precision. The design includes Sliding Mode Controller, PI Controller and High Gain Observer. The Control technique is at first transformed to digital domain using Simulink functional blocks. Simulation results are verified using functional simulation while the control scheme is in discrete form and output of each block is compared with blocks in continuous domain to find out which block is losing accuracy. The Simulink blocks in the design are finally replaced with Xilinx synthesizable blocksets. Functional verification is performed using MATLAB/Simulink as system level testbench.

HDL Co-simulation is also performed to see the waveforms of inputs, outputs, internal registers using third party tool Modelsim of the synthesizable RTL generated by compilation of Xilinx-specific blocksets. Synthesis and timing reports are generated to witness the resources utilized by the complex algorithm and timing closures. This is done using the Xilinx suite ISE project, generated by MATLAB/Simulink while compiling. The project generated, includes the HDL files converted against Xilinx-specific blocksets. This project can be directly used for HDL based functional simulations and generation of bitstream file to be uploaded on specific FPGA variant. The resource utilization for target board Nexy4 DDR is shown in Table 5.1.

Table 5.1: FPGA Resource Utilization

Device Utilization Summary (estimated values)			
Logic Utilization	**Used**	**Available**	**Utilization**
Number of Slice Registers	97	126800	0%
Number of Slice LUTs	2	63400	0%
Number of fully used LUT-FF pairs	1	98	1%
Number of bonded IOBs	130	210	61%
Number of BUFG/BUFGCTRLs	1	32	3%

5.5 FPGA-IN-THE-LOOP (FIL) Simulation Setup

FIL Simulation is useful to verify product functionality in real time. It is a technique to test and validate the design on hardware such as FPGA using Simulink as a testing environment. It can also be termed as Hardware Co-Simulation because the input parameters are fed to FPGA through JTAG/Ethernet from dynamics of the model and output is provided back to dynamics for actuation in terms of control systems as shown in Figure 5.4. In this scenario simulation speeds up because the design is running on dedicated hardware running at fast clock of target FPGA. In our design Simulink sampling frequency is 1.25MHz while the target device clock rate is fixed to 100MHz. Hence sampling rate of FPGA is faster than the Simulink environment, which outputs at very faster rate as compared to the input sampling.

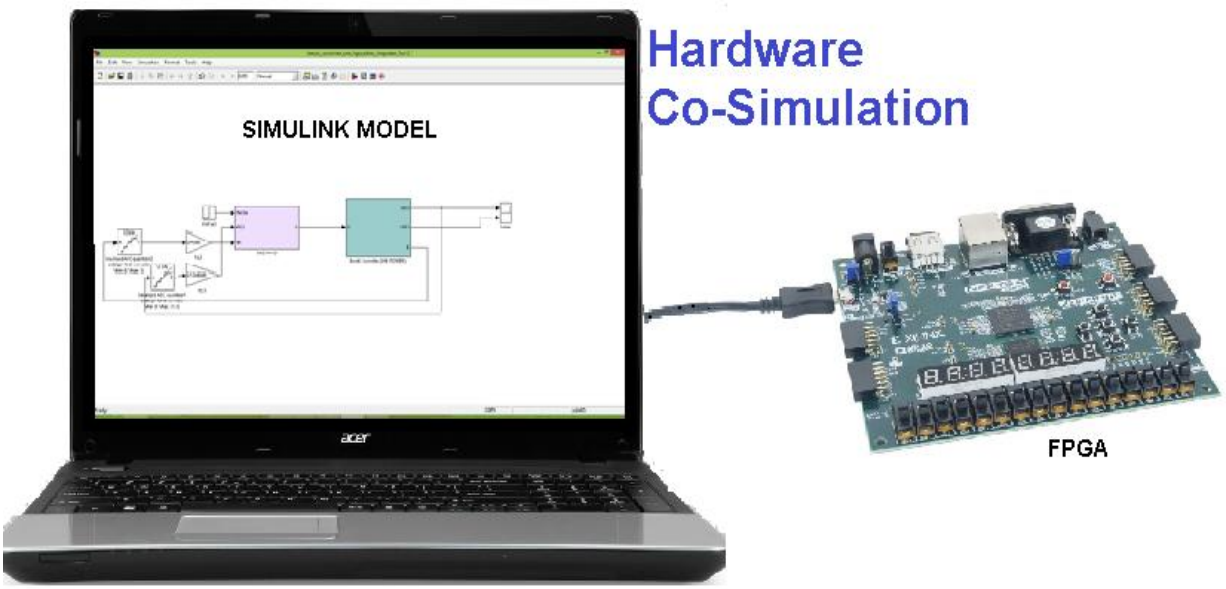

Figure 5.4: FPGA-IN-THE-LOOP Simulation Setup

5.6 FPGA-IN-THE-LOOP(FIL) Simulation Results

Considering DC/DC boost converter parameters initially as V_{in} = 5V, V_{ref} = 12V, L = 330mH and C = 4.7uF, Load resistance R = 820Ω. FPGA-IN-THE-LOOP (FIL) Simulation is performed to verify the estimation of the inductor current using the High Gain Observer. Figure 5.3 shows the tracking of output voltage with respect to the reference voltage while control scheme is running on hardware speeds.

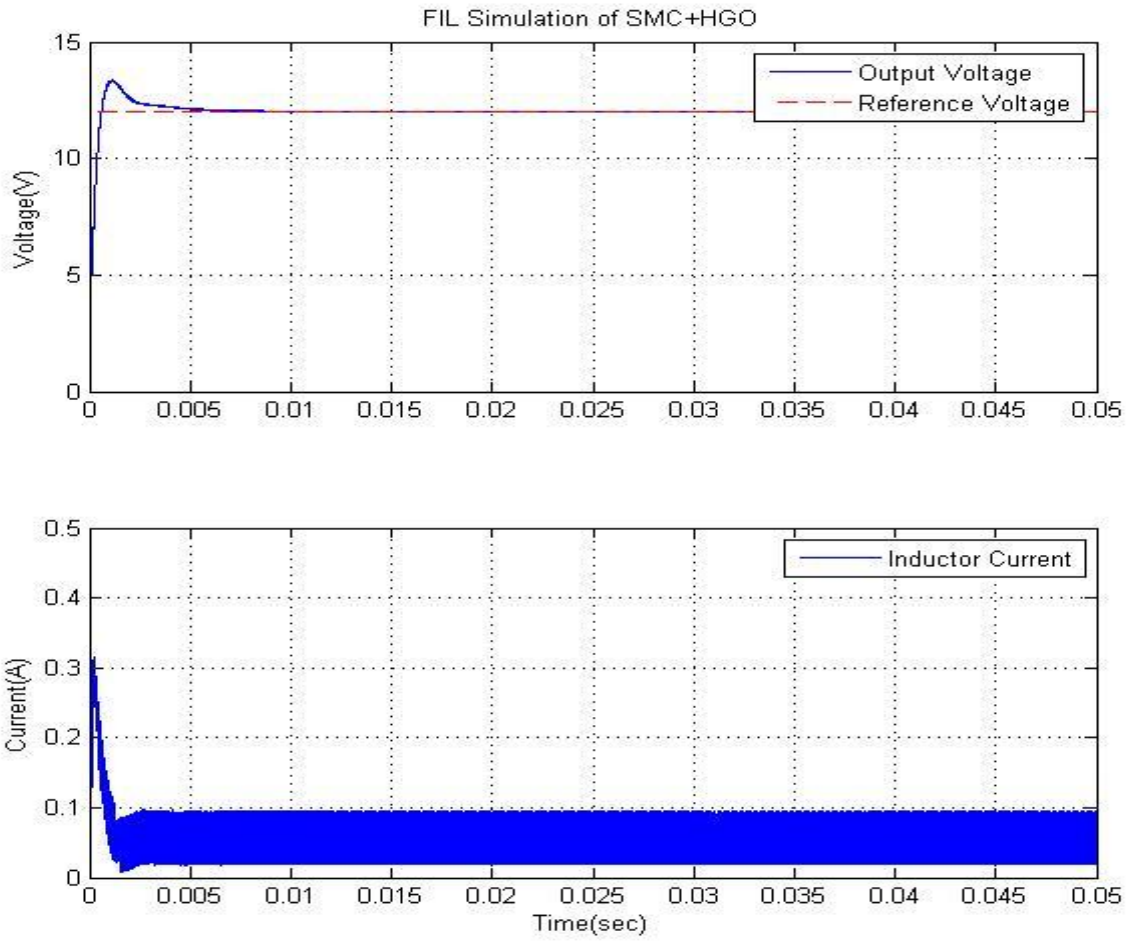

Figure 5.5: FPGA-IN-THE-LOOP Simulation Result

5.7 Conclusion

This chapter discusses the FPGA implementation of the control algorithm proposed in previous chapters. The implementation is done using Xilinx System Generator in

Simulink environment. The FPGA-IN-THE-LOOP(FIL) simulation is performed to ensure the performance of the control scheme on hardware speeds. Hence it shows that the complex algorithms can be easily implemented on FPGA because of its advancements.

\

Chapter 6 Conclusion & Future Recommendations

6.1 Conclusion

In this thesis, Sliding Mode Control design technique is considered for controlling the DC/DC boost converter to maintain the desired output voltage (greater than the input voltage). Stability analysis of controller is also shown through Lyapunav candidate. The controller takes inductor current as a feedback which requires current sensor. Estimation algorithms are included in the design because of the drawbacks of Current Sensors. Therefore, Sliding Mode Observer and High Gain Observer are presented to estimate the inductor current. The transient response of High Gain Observer is shown better than Sliding Mode Observer. Simulation results are provided to evaluate the performance of the sensor-less control scheme.

The Sensor-less control technique which includes controller and observer is implemented on an FPGA for the practical realization on hardware speeds. The implementation aspects on FPGA are also discussed in details. It is shown in FPGA-IN-THE-LOOP (FIL) simulation results, that the proposed control scheme is robust with respect to the load or variations in the input voltage. Hence complex non-linear control algorithms can now easily be implemented on FPGA.

6.2 Future Recommendations

Among the multitude of possible future extensions following are proposed in order to realize a system for a more robust performance for practical applications.

- Our proposed technique can also be applied to other types of the DC/DC Converters such as Buck, Buck-Boost and Cuk converters.
- Different other control techniques can be designed and implemented for DC/DC Converters.
- This work can be extended to the AC/DC Converters.
- The results obtained through FPGA-IN-THE-LOOP (FIL) simulation prove that that design can be taken to next level for product design.

- The sensor-less control technique can also be applied to other applications to eliminate the usage of sensors which can add cost to the product and reduce complexity.

References

[1] Mohan, N., & Undeland, T. M. (2007). *Power electronics: converters, applications, and design*. John Wiley & Sons.

[2] Saravanan, J., Elsi, S. S., & Saravanan, J. (2013). Zero Voltage Switching Of Boost Converter with High Voltage Gain. *Int. Journal of Engineering Research and Applications*, *3*(6), 1921-1926.

[3] Guldemir, H. (2005). Sliding mode control of DC-DC boost converter. *Journal of Applied Sciences*, *5*(3), 588-592.

[4] Tan, S. C., Lai, Y. M., & Chi, K. T. (2008). General design issues of sliding-mode controllers in DC–DC converters. *IEEE Transactions on Industrial Electronics*, *55*(3), 1160-1174.

[5] Jiao, J. (2013). Sliding Mode Control for Stabilizing of Boost Converter in a Solid Oxide Fuel Cell. *Cybernetics and Information Technologies*, *13*(4), 139-147.

[6] Utkin, V., Guldner, J., & Shi, J. (2009). *Sliding mode control in electro-mechanical systems* (Vol. 34). CRC press.

[7] Chen, Z., Gao, W., Hu, J., & Ye, X. (2011). Closed-loop analysis and cascade control of a nonminimum phase boost converter. *IEEE Transactions on power electronics*, *26*(4), 1237-1252.

[8] System Generator for DSP –Getting Started guide,Xilinx,2008

[9] Zhang, Q., Tong, Q., & Zhang, H. (2014, June). An inductor current observer based on improved ekf for dc/dc converter. In *Computer, Consumer and Control (IS3C), 2014 International Symposium on* (pp. 892-895). IEEE.

[10] Pahlevani, M., Pan, S., Eren, S., Bakhshai, A., & Jain, P. (2014). An adaptive nonlinear current observer for boost PFC AC/DC converters. *IEEE Transactions on Industrial Electronics*, *61*(12), 6720-6729.

[11] Makki, A., Bose, S., Giuliante, T., & Walsh, J. (2010, March). Using hall-effect sensors to add digital recording capability to electromechanical relays. In *Protective Relay Engineers, 2010 63rd Annual Conference for* (pp. 1-12). IEEE.

[12] Pankau, J., Leggate, D., Schlegel, D. W., Kerkman, R. J., & Skibiniski, G. L. (1999). High-frequency modeling of current sensors [of IGBT VSI]. *IEEE Transactions on Industry Applications*, *35*(6), 1374-1382.

[13] Honeywell, Application Note, 005715-2-EN IL50 GLO 1198 Hall Effect Sensing and Application, Morristown, NJ, USA, Application Note,005715-2-EN IL50 GLO 1198.

[14] Unitrode Application Note DN-41 P. C. Todd, Extend Current TransformerRange, Unitrode Application Note DN-41.

[15] Qiu, D. Y., Yip, S. C., Chung, H. H., & Hui, S. R. (2003). On the use of current sensors for the control of power converters. *IEEE Transactions on Power Electronics*, *18*(4), 1047-1055.

[16] Bhartiya, P., Rathore, N., & Fulwani, D. (2014, October). A tutorial on implementation of Sliding mode observer for DC/DC power converters using FPGA. In *Industrial Electronics Society, IECON 2014-40th Annual Conference of the IEEE* (pp. 4153-4159). IEEE.

[17] Gonzalez-Fonseca, N., De Leon-Morales, J., & Leyva-Ramos, J. (2005, December). Observer-based controller for switch-mode DC-DC converters. In *Decision and Control, 2005 and 2005 European Control Conference. CDC-ECC'05. 44th IEEE Conference on* (pp. 4773-4778). IEEE.

[18] Wu, Z., & Liu, C. (2010, July). Backstepping design of current-mode controller for DC/DC boost power converters. In *Intelligent Control and Automation (WCICA), 2010 8th World Congress on* (pp. 2103-2106). IEEE.

[19] Kim, S. K., Kim, J. S., Park, C. R., & Lee, Y. I. (2013). Output-feedback model predictive controller for voltage regulation of a DC/DC converter. *IET Control Theory & Applications*, *7*(16), 1959-1968.

[20] Khalil, H. K., & Praly, L. (2014). High-gain observers in nonlinear feedback control. *International Journal of Robust and Nonlinear Control*, *24*(6), 993-1015.

[21] Nexys4DDR™ FPGA Board Reference Manual, Xilinx

[22] Khan, H. S., & Memon, A. Y. (2016, January). FIL simulation of sliding mode controller for DC/DC boost converter. In *Applied Sciences and Technology (IBCAST), 2016 13th International Bhurban Conference on* (pp. 112-117). IEEE.